

# Bayesian Inverse Problems on Metric Graphs

D. Bolin<sup>1</sup>, W. Li<sup>\*,2</sup>, and D. Sanz-Alonso<sup>3</sup>

<sup>1</sup>CEMSE Division, King Abdullah University of Science and Technology, Saudi Arabia

<sup>2</sup>Committee on Computational and Applied Mathematics, University of Chicago, USA

<sup>3</sup>Department of Statistics, University of Chicago, USA

## Abstract

This paper studies the formulation, well-posedness, and numerical solution of Bayesian inverse problems on metric graphs, in which the edges represent one-dimensional wires connecting vertices. We focus on the inverse problem of recovering the diffusion coefficient of a (fractional) elliptic equation on a metric graph from noisy measurements of the solution. Well-posedness hinges on both stability of the forward model and an appropriate choice of prior. We establish the stability of elliptic and fractional elliptic forward models using recent regularity theory for differential equations on metric graphs. For the prior, we leverage modern Gaussian Whittle–Matérn process models on metric graphs with sufficiently smooth sample paths. Numerical results demonstrate accurate reconstruction and effective uncertainty quantification.

**Keywords:** Metric graphs; (fractional) elliptic inverse problems; Bayesian approach; Gaussian Whittle–Matérn processes; well-posedness

## 1 Introduction

Differential equations on metric graphs are used to model diverse phenomena ranging from traffic flow in road networks [5] to wave propagation in thin structures arising in mesoscopic systems, photonic crystals, and nanotechnology [26]. These and other applications motivate the study of inverse problems for differential equations on metric graphs. In this work, we focus on the inverse problem of recovering the diffusion coefficient of a (fractional) elliptic partial differential equation (PDE) from noisy measurements of the solution. Importantly, the unknown to-be-reconstructed diffusion coefficient represents a function defined along the edges of the metric graph.

We will adopt the Bayesian approach to inverse problems [24, 36, 10, 32], placing a prior on the unknown parameter, and conditioning on the observed data to obtain its posterior distribution. In the Bayesian approach, the posterior not only yields point estimators for the unknown parameter, but also enables to quantify the uncertainty in the reconstruction. Furthermore, the Bayesian formulation can result in a form of *well-posedness*, by which small perturbations in the data, the prior, or the forward model yield small perturbations in the posterior [36, 28]. However, well-posedness of Bayesian inversion hinges on both stability of the forward model and an appropriate choice of prior. Ensuring well-posedness is particularly delicate when the to-be-reconstructed parameter is a function, as is the case in this work.

In Euclidean domains, well-posedness of Bayesian inversion in function space has been extensively studied, see e.g. [36, 14, 28] and references therein. The papers [13, 17] established the formulation and well-posedness of elliptic and fractional elliptic inverse problems that have become standard test-beds for theory and methods for Bayesian inversion and uncertainty quantification. More recently, the works [22, 21, 25] studied Bayesian inversion and optimization

---

\*Corresponding author: wenwenli@uchicago.edu

for differential equations on manifolds and point clouds. Relatedly, [16, 18, 19] formulate semi-supervised learning as a Bayesian inverse problem on a graph, where vertices represent labeled and unlabeled features and edges encode similarities between them. In that setting, the goal is to assign labels to all the features, which involves specifying a prior for functions defined on the *vertices* [35], and conditioning on the labeled data to find the posterior.

To our knowledge, this is the first paper to study the formulation and well-posedness of Bayesian inversion on metric graphs. Our goal is to recover a function defined on the *edges* that represents an unknown parameter of a differential equation on a metric graph. Extending the theory from the Euclidean, manifold, and graph settings to the metric graph setting is far from straightforward: the piecewise one-dimensional geometry together with the vertex coupling conditions introduce new regularity and stability challenges. On the other hand, since metric graphs are locally one-dimensional, some classical Euclidean estimates can be improved. We analyze the stability of forward models for elliptic and fractional elliptic inverse problems building on recent regularity theory for differential equations on metric graphs developed in [3]. To ensure well-posedness, we leverage Gaussian Whittle–Matérn prior models on metric graphs with sufficiently smooth sample paths, introduced and analyzed in [9].

The rest of this paper is organized as follows. Section 2 contains background on metric graphs. Section 3 introduces the formulation of Bayesian inversion on metric graphs. Section 4 contains our main technical contributions; we establish continuous dependence (in Hellinger distance) of the posterior distribution on the data by developing new stability theory for forward models on compact metric graphs. Section 5 reports numerical experiments for elliptic and fractional elliptic inverse problems on a letter-shaped metric graph. Our numerical results demonstrate both accurate reconstruction and successful uncertainty quantification. The code is publicly available at: <https://github.com/WenwenLi2002/Bayesian-Inverse-Problems-on-Metric-Graphs>. Finally, Section 6 closes with conclusions and open directions for future research.

## 2 Background

This section introduces necessary background on metric graphs, as well as the function spaces in which we will formulate and analyze Bayesian inversion on metric graphs.

### 2.1 Metric Graphs and Function Spaces

Let  $\Gamma$  be a graph with vertices  $V = \{v_i\}$  and edges  $E = \{e_j\}$ . We are interested in applications where the edges do not represent abstract relationships between vertices, but rather physical one-dimensional wires connecting them. To model this scenario, we assign to each edge  $e \in E$  a positive length  $\ell_e > 0$ , and then we orient each edge arbitrarily and identify it with the interval  $[0, \ell_e]$  via a coordinate  $t_e$ . A graph  $\Gamma$  supplemented with this structure is called a *metric graph*, where the metric is naturally given by the shortest path distance [1]. A generic point  $x$  on a metric graph  $\Gamma$  can be represented as  $x = (e, t_e)$  for some  $e \in E$  and  $t_e \in [0, \ell_e]$ . Thus, points on a metric graph include not only the vertices (for which  $t_e \in \{0, \ell_e\}$ ), but also intermediate points on the edges (for which  $t_e \in (0, \ell_e)$ ). In this paper, we work with *compact metric graphs* comprising finitely many vertices and edges, with every edge of finite length. It can be shown that a metric graph equipped with its natural metric defines a compact metric space [1].

A function  $f$  on a metric graph  $\Gamma$  can be represented as a collection  $\{f_e\}_{e \in E}$ , where  $f_e$  is a function defined on the edge  $e \cong [0, \ell_e]$ . We write

$$\int_{\Gamma} f \, dx := \sum_{e \in E} \int_0^{\ell_e} f_e(t) \, dt.$$

Function spaces on  $\Gamma$  can be defined in terms of function spaces on the edges. For instance, we

let  $L^2(e)$  be the space of Lebesgue square-integrable functions on  $e \cong [0, \ell_e]$  and define

$$L^2(\Gamma) := \bigoplus_{e \in E} L^2(e) = \left\{ f = (f_e)_{e \in E} \mid f_e \in L^2(e), \quad \forall e \in E \right\}, \quad \|f\|_{L^2(\Gamma)}^2 := \sum_{e \in E} \|f_e\|_{L^2(e)}^2.$$

In many applications, we are interested in global functions with additional regularity in each edge. Furthermore, appropriate matching conditions at the vertices —such as continuity or Kirchhoff-type conditions— may be imposed to ensure that the edgewise functions are appropriately connected, resulting in a function on  $\Gamma$  with desired global behavior. Table 2.1 summarizes several function spaces defined on  $\Gamma$  that will be used in this paper. These include spaces defined on each edge and spaces defined on the entire graph, along with their associated norms and dual spaces. Together, these function spaces provide a rigorous framework for studying differential equations on metric graphs.

Table 2.1: Function spaces on  $\Gamma$  and on edges  $e \in E$ .

Notation	Definition	Norm
$H^1(e), e \in E$	See [29, p. 77]	$\ \cdot\ _{H^1(e)}$ (see [29, p. 77])
$H^s(e), e \in E$	See [29, p. 77]	$\ \cdot\ _{H^s(e)}$ (see [29, p. 77])
$H^s(\Gamma), s \in (0, 1)$	$(L^2(\Gamma), H^1(\Gamma))_s$	$\ \cdot\ _{H^s(\Gamma)} := \ \cdot\ _{(L^2(\Gamma), H^1(\Gamma))_s}$
$L^\infty(\Gamma)$	$\{f : \Gamma \rightarrow \mathbb{R} : \ f\ _{L^\infty(\Gamma)} = \text{ess sup}_{x \in \Gamma}  f(x)  < \infty\}$	$\ f\ _{L^\infty(\Gamma)} = \text{ess sup}_{x \in \Gamma}  f(x) $
$C(\Gamma)$	$\{f \in L^2(\Gamma) : f \text{ is continuous on } \Gamma\}$	$\ f\ _{C(\Gamma)} = \sup_{x \in \Gamma}  f(x) $
$C^{0,s}(\Gamma), s \in (0, 1]$	See [9, Section 2]	See [9, Section 2]
$H^1(\Gamma)$	$\{f \in \bigoplus_{e \in E} H^1(e) : f \text{ is continuous on } \Gamma\}$	$\ f\ _{H^1(\Gamma)} = \left( \sum_{e \in E} \ f\ _{H^1(e)}^2 \right)^{1/2}$
$H^{-1}(\Gamma)$	Dual space of $H^1(\Gamma)$	Dual norm
$H^s(\Gamma), s \in (1, 2)$	$(H^1(\Gamma), \tilde{H}_C^2(\Gamma))_{s-1}$	$\ \cdot\ _{H^s(\Gamma)} := \ \cdot\ _{(H^1(\Gamma), \tilde{H}_C^2(\Gamma))_{s-1}}$
$\tilde{H}^s(\Gamma), s \in (0, 1)$	$(L^2(\Gamma), \tilde{H}^1(\Gamma))_s$	$\ \cdot\ _{\tilde{H}^s(\Gamma)} := \ \cdot\ _{(L^2(\Gamma), \tilde{H}^1(\Gamma))_s}$
$\tilde{H}^s(\Gamma), s \in (1, 2)$	$(H^1(\Gamma), \tilde{H}^2(\Gamma))_{s-1}$	$\ \cdot\ _{\tilde{H}^s(\Gamma)} := \ \cdot\ _{(H^1(\Gamma), \tilde{H}^2(\Gamma))_{s-1}}$

Here, for two Hilbert spaces  $\mathcal{H}_1 \subset \mathcal{H}_0$ , we denote by  $(\mathcal{H}_0, \mathcal{H}_1)_s$  the real interpolation of order  $s \in (0, 1)$  between  $\mathcal{H}_0$  and  $\mathcal{H}_1$  using the  $K$ -method —see [9, Appendix A]. Furthermore,  $\tilde{H}^r(\Gamma) = \bigoplus_{e \in E} H^r(e)$  for  $r \in \mathbb{N}$  is a decoupled Sobolev space defined as the direct sum of the corresponding Sobolev spaces on the edges, and  $\tilde{H}_C^r(\Gamma)$  means  $\tilde{H}_C^r(\Gamma) = \tilde{H}^r(\Gamma) \cap C(\Gamma)$  for  $r \in \mathbb{N}$ . We note in particular that the space  $\tilde{H}^1(\Gamma)$  is defined as the decoupled direct sum of  $H^1(e)$  spaces on each edge whereas the space  $H^1(\Gamma)$  requires global continuity over the entire metric graph  $\Gamma$ . This distinction is crucial when studying differential equations on  $\Gamma$ , as the imposition of continuity conditions at the vertices influences the analytical properties of the solutions.

## 2.2 Quantum Graphs

A metric graph is called a *quantum graph* when equipped with a differential operator and appropriate *vertex conditions*. We first introduce a general second-order elliptic differential operator  $\mathcal{L}$  on a compact metric graph  $\Gamma$ . Consider a sufficiently smooth function  $p$  defined on  $\Gamma$ . Locally, on each edge  $e \in E$ , the operator  $\mathcal{L}$  acts on  $p$  by

$$-\frac{d}{dt} \left( a_e(t) \frac{d}{dt} p_e(t) \right) + \kappa_e^2(t) p_e(t), \quad t \in (0, \ell_e), \quad (2.1)$$

where  $p_e$  is the restriction of  $p$  to the edge  $e$ ,  $a_e(t)$  is a Lipschitz and strictly positive function bounded away from zero, and  $\kappa_e(t)$  is bounded and has a strictly positive lower bound.

To formulate a global problem  $\mathcal{L}p = f$  on  $\Gamma$  for some  $f \in L^2(\Gamma)$ , we impose coupling conditions at each vertex. Specifically, we require the solution  $p$  to be continuous at all vertices, and we enforce generalized Kirchhoff-type conditions at vertices given explicitly by

$$p \text{ is continuous on } \Gamma, \quad \text{and} \quad \forall v \in V : \quad \sum_{e \in E_v} a_e(v) \partial_e p(v) = \theta p(v), \quad (2.2)$$

where  $E_v$  is the set of edges incident to vertex  $v$ ,  $\partial_e p(v)$  denotes the outward-directed derivative of  $p$  at vertex  $v$  along edge  $e$ , and  $\theta \in \mathbb{R}$  is a given parameter. The standard Kirchhoff conditions correspond to  $\theta = 0$ , which ensures that flux is conserved at every vertex.

Under these conditions, it has been shown in [3] that the operator  $\mathcal{L}$  defined on  $\Gamma$  possesses a discrete spectrum consisting of eigenvalues  $\{\lambda_j\}_{j=1}^\infty$  in non-decreasing order with corresponding eigenfunctions  $\{\varphi_j\}_{j=1}^\infty$  forming a complete orthonormal basis of  $L^2(\Gamma)$ . Therefore, for  $\beta > 0$ , we can define the fractional power  $\mathcal{L}^\beta$  of the operator  $\mathcal{L}$  via its spectral decomposition as follows:

$$\mathcal{L}^\beta p = \sum_{j=1}^\infty \lambda_j^\beta \langle p, \varphi_j \rangle_{L^2(\Gamma)} \varphi_j, \quad p \in \mathcal{D}(\mathcal{L}^\beta),$$

where  $\mathcal{D}(\mathcal{L}^\beta)$  is the natural domain of  $\mathcal{L}^\beta$ , and  $\langle f, g \rangle_{L^2(\Gamma)} = \int_\Gamma f g \, dx$  is the  $L_2(\Gamma)$  inner product. This leads to the fractional elliptic differential equation

$$\mathcal{L}^\beta p = f \quad \text{on } \Gamma,$$

with given  $f \in L^2(\Gamma)$ , which we will study in detail below.

### 3 Inverse Problem Formulation

Let  $\Gamma$  be, here and throughout, a compact metric graph. For given  $\beta \geq 1$ , consider the (fractional) elliptic differential equation:

$$\mathcal{L}_u^\beta p := \left( \kappa^2 - \nabla \cdot (e^u \nabla) \right)^\beta p = f \quad \text{on } \Gamma, \quad (3.1)$$

where  $\mathcal{L}_u$  is equipped with the Kirchhoff vertex conditions (2.2) with  $a_e = \exp(u_e)$ , and  $f \in L^2(\Gamma)$  represents a given source term. For convenience, we only consider the standard Kirchhoff vertex condition ( $\theta = 0$  in Equation 2.2) and constant coefficient  $\kappa > 0$ . We will refer to  $\beta = 1$  as the *elliptic case* and to  $\beta > 1$  as the *fractional case*. Our goal is to find the unknown function  $u$  specifying the diffusion coefficient of  $\mathcal{L}_u$  from noisy measurements of the solution  $p$ .

**Proposition 3.1** (Existence and Uniqueness of Solutions). *If  $u \in H^{3/2}(\Gamma)$ , then  $\exp(u)$  is a positive Lipschitz function on  $\Gamma$ , and for every  $f \in L^2(\Gamma)$  the equation (3.1) admits a unique solution  $p \in H^1(\Gamma)$ .*

*Proof.* To prove that  $\exp(u)$  is Lipschitz, we must show that there exists  $c > 0$  such that for all  $x, x' \in \Gamma$ ,  $|\exp(u(x)) - \exp(u(x'))| \leq c \cdot d(x, x')$ , where  $d(\cdot, \cdot)$  denotes the natural metric on  $\Gamma$ . If  $x, x'$  are on the same edge  $e \cong [0, \ell_e]$ , a point  $\xi$  between  $x$  and  $x'$  exists such that

$$|\exp(u(x)) - \exp(u(x'))| \leq |\exp(\xi) u'(\xi)| d(x, x'), \quad (3.2)$$

by the mean value theorem. Further, the one-dimensional Sobolev embedding

$$H^{3/2}(0, \ell_e) \hookrightarrow C^{0,1}[0, \ell_e]$$

implies that constants  $M_e, c_e > 0$  exist such that  $\|u_e\|_{L^\infty(e)} < M_e$  and  $\|u'_e\|_{L^\infty(e)} < c_e$ . Define  $c = \sup_e \exp(M_e) c_e$ , which is finite as the graph is compact. Using that  $|\exp(\xi) u'(\xi)| < \exp(M_e) c_e \leq c$  in (3.2) gives the result.

If  $x, x'$  are on different edges, suppose that a shortest path from  $x$  to  $x'$  goes through  $n$  vertices  $v_1, \dots, v_n$ . Because  $u \in H^{3/2}(\Gamma)$ ,  $u$  is continuous at the vertices, and the triangle inequality gives that

$$|e^{u(x)} - e^{u(x')}| \leq |e^{u(x)} - e^{u(v_1)}| + \sum_{i=1}^{n-1} |e^{u(v_{i+1})} - e^{u(v_i)}| + |e^{u(v_n)} - e^{u(x')}|.$$

Using the result for locations on the same edge on each term in this sum gives the result.

Since  $\exp(u)$  is a positive Lipschitz function, then [3, Proposition 3.1] guarantees the existence and uniqueness of a solution  $p \in H^1(\Gamma)$  to (3.1) both in the classical and fractional cases.  $\square$

Thanks to Proposition 3.1, we can define the *forward map* from parameter  $u$  to solution  $p$ :

$$\begin{aligned} \mathcal{F} : H^{3/2}(\Gamma) &\rightarrow H^1(\Gamma), \\ u &\mapsto p. \end{aligned} \tag{3.3}$$

We assume to have access to  $m$  noisy measurements of  $p$  of the form

$$y_j = l_j(p) + \eta_j, \quad j = 1, \dots, m, \tag{3.4}$$

where  $\{\eta_j\}_{j=1}^m$  represent measurement errors, not necessarily independent. We consider two cases:

**Data Assumption 3.2.**  $\{l_j\}_{j=1}^m$  are bounded linear functionals on  $H^1(\Gamma)$ .

**Data Assumption 3.3.**  $\{l_j\}_{j=1}^m$  are pointwise measurements, so that  $l_j(p) = p(x_j)$  for  $x_j \in \Gamma$ .

In either case, we define the *observation map*

$$\begin{aligned} \mathcal{Q} : H^{3/2}(\Gamma) &\rightarrow \mathbb{R}^m, \\ p &\mapsto (l_1(p), \dots, l_m(p))^\top, \end{aligned}$$

and we refer to the operator  $\mathcal{G} := \mathcal{Q} \circ \mathcal{F} : H^{3/2}(\Gamma) \rightarrow \mathbb{R}^m$  obtained by composing the observation and forward maps as the *forward model*. Concatenating the observations, we then have

$$y = \mathcal{G}(u) + \eta, \tag{3.5}$$

where  $y = (y_1, \dots, y_m)^\top$  and  $\eta = (\eta_1, \dots, \eta_m)^\top$ . We assume that the measurement noise is centered Gaussian with positive definite covariance  $\Sigma$ , written  $\eta \sim \mathcal{N}(0, \Sigma)$ .

Our goal is to recover the unknown parameter  $u \in H^{3/2}(\Gamma)$  from the data  $y \in \mathbb{R}^m$  using the Bayesian approach to inverse problems [24, 36, 14, 10, 32]. To that end, we will specify a *prior distribution* on  $u$  and combine it with the *likelihood function* determined by (3.5) to obtain the *posterior distribution* of  $u$  given  $y$ . In the Bayesian framework, the posterior distribution is used to obtain point estimates for  $u$  and quantify the uncertainty in the reconstruction [32]. However, in our metric graph setting a careful choice of prior distribution will be essential to rigorously justify that the posterior distribution is a well-defined probability measure, which can be written as a change of measure with respect to the prior. We introduce and motivate our choice of prior in Subsection 3.1. Next, we define the likelihood function in Subsection 3.2. Finally, we formally derive the posterior distribution in Subsection 3.3. In Section 4, we will rigorously show that the posterior distribution is well defined and stable with respect to perturbations in the data.

### 3.1 Prior Distribution

We will take the prior distribution to be the law of a (generalized) Whittle-Matérn Gaussian process on the metric graph [9, 3]. Specifically, we set the prior to be  $\mu_0 = \text{Law}(u)$ , where  $u$  is the solution of the fractional stochastic PDE

$$\left(\kappa_0^2 - \nabla \cdot (a \nabla)\right)^\alpha u = \mathcal{W}. \quad (3.6)$$

Here,  $\kappa_0 \in L^\infty(\Gamma)$  is assumed to satisfy  $\text{ess inf}_{x \in \Gamma} \kappa_0(x) \geq c > 0$  for some constant  $c > 0$ ,  $a : \Gamma \rightarrow \mathbb{R}$  is a positive Lipschitz function,  $\kappa_0^2 - \nabla \cdot (a \nabla)$  is equipped with Kirchhoff vertex conditions, the fractional operator  $\left(\kappa_0^2 - \nabla \cdot (a \nabla)\right)^\alpha$  is defined spectrally, the exponent  $\alpha > 0$  controls the regularity of solution, and  $\mathcal{W}$  denotes Gaussian white noise on  $\Gamma$ . We recall that if  $\{e_k\}_{k \in \mathbb{N}}$  is an orthonormal basis of  $L^2(\Gamma)$  (its existence is guaranteed by the compactness of  $\Gamma$ ), then the white noise  $\mathcal{W}$  can be represented by the series

$$\mathcal{W} = \sum_{k \in \mathbb{N}} \xi_k e_k,$$

where  $\{\xi_k\}_{k \in \mathbb{N}}$  is a sequence of independent, real-valued standard normal random variables.

**Proposition 3.4** (Regularity of Prior Gaussian Process (See [3])). *Let  $u$  be the solution of (3.6), where the operator is equipped with Kirchhoff vertex conditions and the coefficients  $a$  and  $\kappa_0$  satisfy the assumptions above. Then,  $u \in H^1(\Gamma)$   $\mathbb{P}$ -a.s. if and only if  $\alpha > \frac{3}{4}$ . Moreover, for any  $\varepsilon > 0$  and any  $\frac{1}{4} \leq \alpha \leq 2 + \frac{1}{4}$ , the sample paths of  $u$  belong to  $\tilde{H}^{2\alpha - \frac{1}{2} - \varepsilon}$   $\mathbb{P}$ -a.s.*

**Remark 3.5.** The condition  $\alpha > 1$  ensures that the sample paths of  $u$  belong to  $H^{3/2}(\Gamma)$   $\mathbb{P}$ -a.s., which exactly meets the regularity requirement on the input parameter in Proposition 3.1 for existence and uniqueness of solutions. Indeed, from Table 2.1, for  $s \in (1, 2)$ , we have

$$\tilde{H}^s(\Gamma) = (\tilde{H}^1(\Gamma), \tilde{H}^2(\Gamma))_{s-1}, \quad H^s(\Gamma) = (H^1(\Gamma), \tilde{H}_C^2(\Gamma))_{s-1},$$

where the only difference between the interpolated spaces  $\tilde{H}^s(\Gamma)$  and  $H^s(\Gamma)$  is global continuity. Since  $\alpha > \frac{3}{4}$  already implies that  $u \in H^1(\Gamma)$  almost surely—and hence that  $u$  is continuous—the additional regularity from  $\alpha > 1$  yields

$$u \in H^1(\Gamma) \cap \tilde{H}^{3/2}(\Gamma) = H^{3/2}(\Gamma) \quad \text{a.s.}$$

In the boundary case  $\alpha = 1$ , sample paths of  $u$  belong  $\mathbb{P}$ -a.s. to  $H^{3/2-\varepsilon}(\Gamma)$ , for any  $\varepsilon > 0$ , corresponding to an  $\varepsilon$ -decay in the Hölder continuity exponent of  $\exp(u)$  (i.e.  $\exp(u) \in C^{0,1-\varepsilon}(\Gamma)$  for all  $\varepsilon > 0$ ). We claim that the existence and uniqueness of the weak solution  $p$  to Equation 3.1 extend to  $u \in H^{3/2-\varepsilon}(\Gamma)$  and that our analysis in Section 4.1 still holds for  $\alpha = 1$ . To justify this claim, we verify that the key properties of the operator  $\mathcal{L}_u$  that underpin our analysis (self-adjointness, positive definiteness with a compact inverse, and a discrete spectrum) still hold with this weaker regularity of  $u$ , and that Weyl's law is also still applicable. First, [27, Theorem 5] shows that  $\mathcal{L}_u$  remains self-adjoint with  $\exp(u) \in C^{0,1-\varepsilon}(\Gamma)$  under Kirchhoff vertex conditions. Second, the compactness of  $\Gamma$  and the positivity of  $\exp(u)$  ensure that  $\mathcal{L}_u$  is positive definite. Third, using the Rellich-Kondrachov compactness theorem, it is straightforward to show that  $\mathcal{L}_u$  has a compact inverse and discrete spectrum. Next, applying Lax's theorem, we directly deduce the existence and uniqueness of the solution  $p$  for Equation 3.1 in  $H^1(\Gamma)$ , which guarantees that the forward map (3.3) is well defined. Finally, [15, Theorem 6.3.1] shows that Weyl's law still holds provided that  $\kappa$  and  $\exp(u)$  are bounded away from zero.  $\square$

### 3.2 Likelihood Function

Building on the data generating process described above, we now define the likelihood function and introduce the corresponding potential function. Since the data  $y$  take values in  $\mathbb{R}^m$  and the noise  $\eta$  is modeled as a mean-zero Gaussian random vector with covariance matrix  $\Sigma \in \mathbb{R}^{m \times m}$ , we define the potential function by

$$\Phi(u; y) := \frac{1}{2} (y - \mathcal{G}(u))^\top \Sigma^{-1} (y - \mathcal{G}(u)) =: \frac{1}{2} \|y - \mathcal{G}(u)\|_{\Sigma^{-1}}^2, \quad (3.7)$$

where, recall,  $\mathcal{G}$  denotes the forward model. Then, the likelihood of  $y$  given  $u$  can be expressed as

$$\pi(y | u) \propto \exp(-\Phi(u; y)).$$

**Remark 3.6.** Our problem formulation and analysis can be readily extended to settings where the data are infinite-dimensional. However, we will restrict our attention to finite-dimensional data, as this setting often occurs in applications.  $\square$

### 3.3 Posterior Distribution

Combining via Bayes' formula the Gaussian Whittle–Matérn prior distribution  $\mu_0$  introduced in Subsection 3.1 with the likelihood function introduced in Subsection 3.2, we can formally derive the posterior distribution  $\mu^y$  of  $u$  given  $y$ , which can be expressed as

$$\frac{d\mu^y}{d\mu_0}(u) \propto \exp(-\Phi(u; y)). \quad (3.8)$$

The fact that the posterior distribution  $\mu^y$  is given by a change of measure with respect to the prior as expressed in (3.8) will be rigorously established in the next section, where we also show the continuous dependence of the posterior on the data in Hellinger distance.

## 4 Well-posedness Theory

This section establishes the well-posedness of the Bayesian inverse problem introduced in Section 3. The main result is Theorem 4.5, which establishes the existence and uniqueness of the posterior distribution, as well as its stability with respect to perturbations in the data. The proof of Theorem 4.5 relies on a careful study of the stability of the forward map (Theorem 4.1) and the forward model (Theorem 4.3).

### 4.1 Main Results

The main technical contribution of this paper is the following stability result for the forward map of elliptic ( $\beta = 1$ ) and fractional elliptic ( $\beta > 1$ ) inverse problems. We recall that  $\alpha$  controls the regularity of samples from the prior  $\mu_0$  introduced in Subsection 3.1 (c.f. Proposition 3.4), and  $f$  denotes the right-hand side of the differential equation (3.1). The proof of Theorem 4.1 is deferred to Subsection 4.2.

**Theorem 4.1 (Stability of the Forward Map).** *Let  $\alpha > 1$ ,  $\beta \geq 1$ , and  $f \in L^2(\Gamma)$ . Then, there exists a constant*

$$c(\beta) = c(\beta, \|f\|_{L^2(\Gamma)}, \Gamma),$$

*decreasing with respect to  $\beta$ , such that, for almost all  $u, u_1, u_2 \sim \mu_0$ :*

$$\|\mathcal{F}(u)\|_V \leq c(\beta) \exp(\beta \|u\|_{L^\infty(\Gamma)}), \quad (4.1)$$

$$\|\mathcal{F}(u_1) - \mathcal{F}(u_2)\|_V \leq c(\beta) \exp\left((\beta + 2) \max\{\|u_1\|_{L^\infty(\Gamma)}, \|u_2\|_{L^\infty(\Gamma)}\}\right) \|u_1 - u_2\|_{L^\infty(\Gamma)}, \quad (4.2)$$

*where  $\|\cdot\|_V = \|\cdot\|_{H^1(\Gamma)}$  or  $\|\cdot\|_V = \|\cdot\|_{L^\infty(\Gamma)}$ .*



**Remark 4.2.** Since compact metric graphs are locally one-dimensional, it suffices to establish the bounds (4.1) and (4.2) for the  $H^1(\Gamma)$  norm. To see this, notice that each edge  $e \in E$  is isometric to a real interval, so the classical one-dimensional Sobolev embedding

$$H^1(e) \hookrightarrow C(e), \quad \|p\|_{L^\infty(e)} \leq c(e) \|p\|_{H^1(e)}$$

applies edge-wise. Enforcing continuity at the vertices then yields the global embedding

$$H^1(\Gamma) \hookrightarrow L^\infty(\Gamma), \quad \|p\|_{L^\infty(\Gamma)} \leq c(\Gamma) \|p\|_{H^1(\Gamma)}.$$

As a result, bounds in the  $H^1(\Gamma)$  norm transfer immediately to the  $L^\infty(\Gamma)$  norm. This control of the  $L^\infty(\Gamma)$  norm by the  $H^1(\Gamma)$  norm holds even when the metric graph  $\Gamma$  is embedded in  $\mathbb{R}^d$ ,  $d \geq 2$ , while the conclusion fails in high-dimensional Euclidean domains.  $\square$

The stability of the forward map, along with our assumptions on the observation map encoded in Data Assumptions 3.2 and 3.3 imply the following stability result for the forward model.

**Theorem 4.3 (Stability of the Forward Model).** *In the setting of Theorem 4.1 and under Data Assumption 3.2 or 3.3, there exists a constant*

$$c(\beta) = c(\beta, \|f\|_{L^2(\Gamma)}, \Gamma, \max_j \|l_j\|_{H^{-1}(\Gamma)}),$$

decreasing with respect to  $\beta$ , such that, for almost all  $u, u_1, u_2 \sim \mu_0$ :

$$\|\mathcal{G}(u)\| \leq c(\beta) \exp(\beta \|u\|_{L^\infty(\Gamma)}), \quad (4.3)$$

$$\|\mathcal{G}(u_1) - \mathcal{G}(u_2)\| \leq c(\beta) \exp\left((\beta + 2) \max\{\|u_1\|_{L^\infty(\Gamma)}, \|u_2\|_{L^\infty(\Gamma)}\}\right) \|u_1 - u_2\|_{L^\infty(\Gamma)}. \quad (4.4)$$

*Proof.* By Theorem 4.1, there exists a constant  $\tilde{c}(\beta)$ , independent of  $u$ , such that:

$$\begin{cases} \|p\|_{H^1(\Gamma)} \leq \tilde{c}(\beta) \exp(\beta \|u\|_{L^\infty(\Gamma)}), \\ \|p_1 - p_2\|_{H^1(\Gamma)} \leq \tilde{c}(\beta) \exp\left((\beta + 2) \max\{\|u_1\|_{L^\infty(\Gamma)}, \|u_2\|_{L^\infty(\Gamma)}\}\right) \|u_1 - u_2\|_{L^\infty(\Gamma)}, \end{cases} \quad (4.5)$$

where  $p_1$  and  $p_2$  denote the solutions to (3.1) corresponding to  $u_1$  and  $u_2$ , respectively.

Since each  $l_j$  is a bounded linear functional on  $H^1(\Gamma)$ , the Riesz representation theorem implies that  $|l_j(p)| \leq \|l_j\|_{H^{-1}} \|p\|_{H^1}$  for  $j = 1, \dots, m$ . Applying the observation map to the solution  $p$  and the difference  $p_1 - p_2$  respectively, we obtain that

$$\begin{cases} \|\mathcal{G}(u)\| \leq \|l\|_{H^{-1}(\Gamma)} \|p\|_{H^1(\Gamma)}, \\ \|\mathcal{G}(u_1) - \mathcal{G}(u_2)\| = \sqrt{\sum_{j=1}^m |l_j(p_1 - p_2)|^2} \leq \sqrt{\sum_{j=1}^m \|l_j\|_{H^{-1}}^2} \|p_1 - p_2\|_{H^1(\Gamma)}. \end{cases} \quad (4.6)$$

Hence, it follows from (4.5) that there exists a constant  $c(\beta) := c(\beta, \|f\|_{L^2(\Gamma)}, \Gamma, \max_j \|l_j\|_{H^{-1}(\Gamma)})$  such that:

$$\begin{cases} \|\mathcal{G}(u)\|_{H^1(\Gamma)} \leq c(\beta) \exp(\beta \|u\|_{L^\infty(\Gamma)}), \\ \|\mathcal{G}(u_1) - \mathcal{G}(u_2)\| \leq c(\beta) \exp\left((\beta + 2) \max\{\|u_1\|_{L^\infty(\Gamma)}, \|u_2\|_{L^\infty(\Gamma)}\}\right) \|u_1 - u_2\|_{L^\infty(\Gamma)}, \end{cases}$$

establishing the boundedness and Lipschitz continuity of the forward model.  $\square$

We will use the Hellinger distance to quantify the proximity between posterior distributions  $\mu^y$  and  $\mu^{y'}$  corresponding to different realizations  $y$  and  $y'$  of the data.



**Definition 4.4** (Hellinger Distance). For two probability measures  $\nu_1$  and  $\nu_2$  on the same measurable space  $(X, \mathcal{B})$ , their *Hellinger distance* is defined as

$$d_H(\nu_1, \nu_2) := \left( \frac{1}{2} \int_X \left( \sqrt{\frac{d\nu_1}{d\nu}} - \sqrt{\frac{d\nu_2}{d\nu}} \right)^2 d\nu \right)^{1/2},$$

where  $\nu$  is a reference measure that dominates both  $\nu_1$  and  $\nu_2$ .

The following is the main result of this section.

**Theorem 4.5** (Well-posedness of the Bayesian Inverse Problem). *Let  $\mu_0$  be the Gaussian Whittle–Matérn prior defined in Subsection 3.1 with regularity parameter  $\alpha > 1$ . For every  $\beta \geq 1$  and measurement  $y \in \mathbb{R}^m$ , define the posterior probability measure  $\mu^y$  on  $\mathbb{R}^m$  by*

$$\frac{d\mu^y}{d\mu_0}(u) = \frac{1}{Z(y)} \exp(-\Phi(u; y)), \quad Z(y) := \int_{H^{3/2}(\Gamma)} \exp(-\Phi(u; y)) d\mu_0(u), \quad (4.7)$$

where the potential  $\Phi: H^{3/2}(\Gamma) \times \mathbb{R}^m \rightarrow \mathbb{R}$  is given by (3.7). Then, the following holds:

- (i) **Well-definedness.**  $\mu^y$  is a well-defined probability measure on  $H^{3/2}(\Gamma)$ .
- (ii) **Stability with respect to the data.** For every radius  $r > 0$ , there exists a constant  $c = c(r) > 0$  such that, for all  $y, y' \in \mathbb{R}^m$  with  $\max\{\|y\|, \|y'\|\} \leq r$ ,

$$d_H(\mu^y, \mu^{y'}) \leq c(r) \|y - y'\|. \quad (4.8)$$

*Proof.* According to [13], if the potential  $\Phi(u, y)$  satisfies the following properties:

- (I) For every  $\epsilon > 0$  and  $r > 0$ , there exists  $M = M(\epsilon, r) \in \mathbb{R}$  such that, for all  $u \in H^{3/2}(\Gamma)$  and for all  $y \in \mathbb{R}^m$  with  $\|y\| < r$ ,

$$\Phi(u, y) \geq M - \epsilon \|u\|_{H^{3/2}(\Gamma)}^2;$$

- (II) For every  $r > 0$ , there exists  $K = K(r) > 0$  such that, for all  $u \in H^{3/2}(\Gamma)$  and for all  $y \in \mathbb{R}^m$  with  $\max\{\|u\|_{H^{3/2}(\Gamma)}, \|y\|\} < r$ ,

$$\Phi(u, y) \leq K;$$

- (III) For every  $r > 0$ , there exists  $L = L(r) > 0$  such that, for all  $u_1, u_2 \in H^{3/2}(\Gamma)$  and for all  $y \in \mathbb{R}^m$  with  $\max\{\|u_1\|_{H^{3/2}(\Gamma)}, \|u_2\|_{H^{3/2}(\Gamma)}, \|y\|\} < r$ ,

$$|\Phi(u_1, y) - \Phi(u_2, y)| \leq L \|u_1 - u_2\|_{H^{3/2}(\Gamma)};$$

- (IV) For every  $\epsilon > 0$  and  $r > 0$ , there exists  $c = c(\epsilon, r) \in \mathbb{R}$  such that, for all  $y_1, y_2 \in \mathbb{R}^m$  with  $\max\{\|y_1\|, \|y_2\|\} < r$  and for every  $u \in H^{3/2}(\Gamma)$ ,

$$|\Phi(u, y_1) - \Phi(u, y_2)| \leq \exp\left(\epsilon \|u\|_{H^{3/2}(\Gamma)}^2 + c\right) \|y_1 - y_2\|,$$

and if  $\mu_0(H^{3/2}(\Gamma)) = 1$ , then the posterior measure  $\mu^y$  defined in (4.7) is well defined and depends Lipschitz continuously on the data  $y$ , as expressed in (4.8). We now verify that these properties hold in our setting. Throughout the proof, we regard the metric graph  $\Gamma$ , the covariance matrix  $\Sigma$  in (3.5), and the parameter  $\beta$  in (3.1) as fixed. Accordingly, we allow the constants to implicitly depend on these parameters.

First, since  $\Phi(u, y) \geq 0$  for all  $u, y$ , we may simply set  $M(\epsilon, r) = 0$ , to verify property (I). Next, under both Data Assumptions 3.2 and 3.3—that is, whether  $\mathcal{G}(u) = \mathcal{Q}(p) = (l_1(p), \dots, l_m(p))^\top$  with each  $l_j$  being a bounded linear functional or a pointwise evaluation of  $p$ —the following inequality holds for any  $(u, y) \in H^{3/2}(\Gamma) \times \mathbb{R}^m$  satisfying  $\max\{\|u\|_{H^{3/2}(\Gamma)}, \|y\|\} < r$ :

$$\begin{aligned}
\Phi(u, y) &= \frac{1}{2} \|y - \mathcal{G}(u)\|_{\Sigma^{-1}}^2 \leq \frac{1}{2} (\|y\|_{\Sigma^{-1}} + \|\mathcal{G}(u)\|_{\Sigma^{-1}})^2 \\
&\leq \frac{1}{2} (\|\Sigma^{-1}\|_{\text{op}} r + \|\Sigma^{-1}\|_{\text{op}} \|\mathcal{G}(u)\|)^2 \\
&\stackrel{(i)}{\leq} \frac{1}{2} (\|\Sigma^{-1}\|_{\text{op}} r + \|\Sigma^{-1}\|_{\text{op}} C_1 e^{\beta\|u\|_{L^\infty(\Gamma)}})^2 \\
&\stackrel{(ii)}{\leq} \frac{1}{2} (\|\Sigma^{-1}\|_{\text{op}} r + C_1 \|\Sigma^{-1}\|_{\text{op}} e^{\beta C_2 \|u\|_{H^{3/2}(\Gamma)}})^2 \\
&\leq \frac{1}{2} (\|\Sigma^{-1}\|_{\text{op}} r + C_1 \|\Sigma^{-1}\|_{\text{op}} e^{\beta C_2 r})^2 =: K(r).
\end{aligned} \tag{4.9}$$

Here, inequality (i) follows from Theorem 4.3, while inequality (ii) uses the Sobolev embedding  $H^{3/2}(\Gamma) \hookrightarrow L^\infty(\Gamma)$ . Hence, we have shown that property (II) holds.

We now seek to verify property (III). Let  $y \in \mathbb{R}^m$  be fixed and given. For  $u \in H^{3/2}(\Gamma)$ , we denote

$$a(u) := \|y - \mathcal{G}(u)\|_{\Sigma^{-1}}.$$

Then, for any given  $u_1, u_2 \in H^{3/2}(\Gamma)$  the elementary identity  $a^2 - b^2 = (a - b)(a + b)$  implies

$$\begin{aligned}
|\Phi(u_1, y) - \Phi(u_2, y)| &= \frac{1}{2} |a(u_1)^2 - a(u_2)^2| = \frac{1}{2} |a(u_1) - a(u_2)| (a(u_1) + a(u_2)) \\
&\leq \frac{1}{2} \|\mathcal{G}(u_1) - \mathcal{G}(u_2)\|_{\Sigma^{-1}} (\|y - \mathcal{G}(u_1)\|_{\Sigma^{-1}} + \|y - \mathcal{G}(u_2)\|_{\Sigma^{-1}}) \\
&\leq \frac{1}{2} \|\Sigma^{-1}\|_{\text{op}} \|\mathcal{G}(u_1) - \mathcal{G}(u_2)\| (\|y - \mathcal{G}(u_1)\|_{\Sigma^{-1}} + \|y - \mathcal{G}(u_2)\|_{\Sigma^{-1}}),
\end{aligned} \tag{4.10}$$

where we have used the reverse triangle inequality. To verify property (III), suppose that  $\max\{\|u_i\|_{H^{3/2}(\Gamma)}, \|y\|\} \leq r$  ( $i = 1, 2$ ). According to property (II), there exists a constant  $c(r) > 0$  such that

$$\|y - \mathcal{G}(u_i)\|_{\Sigma^{-1}} \leq c(r), \quad (i = 1, 2). \tag{4.11}$$

Applying Theorem 4.3 yields a constant  $L_1(r) > 0$  such that

$$\begin{aligned}
\|\mathcal{G}(u_1) - \mathcal{G}(u_2)\| &\stackrel{(iii)}{\leq} C_3 \exp((\beta + 2)\|u_1 - u_2\|_{L^\infty(\Gamma)}) \\
&\stackrel{(iv)}{\leq} C_3 \exp((\beta + 2)C_4\|u_1 - u_2\|_{H^{3/2}(\Gamma)}) \\
&\leq L_1(r) \|u_1 - u_2\|_{H^{3/2}(\Gamma)},
\end{aligned} \tag{4.12}$$

where (iii) follows from Theorem 4.3, and (iv) can be obtained by applying the Sobolev embedding theorem on  $L^\infty(\Gamma)$ . Inserting (4.11) and (4.12) into (4.10) gives

$$|\Phi(u_1, y) - \Phi(u_2, y)| \leq \|\Sigma^{-1}\|_{\text{op}} c(r) L_1(r) \|u_1 - u_2\|_{H^{3/2}(\Gamma)} =: L(r) \|u_1 - u_2\|_{H^{3/2}(\Gamma)},$$

where  $L(r) := c(r)L_1(r)$ , implying that property (III) holds.

To verify property (IV), fix  $u \in H^{3/2}(\Gamma)$  and let  $y_1, y_2 \in \mathbb{R}^m$  satisfy  $\max\{\|y_1\|, \|y_2\|\} \leq r$ . A

direct expansion gives

$$\begin{aligned}
|\Phi(u, y_1) - \Phi(u, y_2)| &= \frac{1}{2} |(y_1 - y_2)^\top \Sigma^{-1} (y_1 + y_2 - 2\mathcal{G}(u))| \\
&\leq \|y_1 - y_2\| \|\Sigma^{-1}\|_{\text{op}} \left( \frac{1}{2} \|y_1 + y_2\| + \|\mathcal{G}(u)\| \right) \\
&\leq \|y_1 - y_2\| \|\Sigma^{-1}\|_{\text{op}} (r + \|\mathcal{G}(u)\|) \\
&\leq \|y_1 - y_2\| \|\Sigma^{-1}\|_{\text{op}} (r + A e^{\beta\|u\|_{L^\infty(\Gamma)}}),
\end{aligned} \tag{4.13}$$

where in the third line we used that  $\frac{1}{2}\|y_1 + y_2\| \leq r$  by hypothesis, and in the last line we applied Theorem 4.3 to bound  $\|\mathcal{G}(u)\| \leq A e^{\beta\|u\|_{L^\infty(\Gamma)}}$ .

For any given  $\varepsilon > 0$ , the inequality  $e^{ts} \leq \exp(\varepsilon s^2 + t^2/(4\varepsilon))$  holds for any  $s \geq 0$  and  $t > 0$ . Hence, by the Sobolev embedding theorem,

$$\|\mathcal{G}(u)\| \leq A \exp(\beta C_5 \|u\|_{H^{3/2}(\Gamma)}) \leq A \exp\left(\varepsilon \|u\|_{H^{3/2}(\Gamma)}^2 + \frac{(\beta C_5)^2}{4\varepsilon}\right).$$

Inserting the previous estimates into (4.13), we obtain

$$\begin{aligned}
|\Phi(u, y_1) - \Phi(u, y_2)| &\leq \|y_1 - y_2\| \|\Sigma^{-1}\|_{\text{op}} \left( r + A \exp\left(\varepsilon \|u\|_{H^{3/2}(\Gamma)}^2 + \frac{(\beta C_5)^2}{4\varepsilon}\right) \right) \\
&\leq \exp\left(\varepsilon \|u\|_{H^{3/2}(\Gamma)}^2 + c(\varepsilon, r)\right) \|y_1 - y_2\|,
\end{aligned}$$

where the constant

$$c(\varepsilon, r) = \log\left(\|\Sigma^{-1}\|_{\text{op}} \left( r + A e^{(C_5 \beta)^2/(4\varepsilon)} \right)\right)$$

depends only on  $(\varepsilon, r)$ . Thus, properties (I)–(IV) are satisfied in our setting. Moreover, it is straightforward to verify that  $\mu_0(H^{3/2}(\Gamma)) = 1$ , which directly follows from Proposition 3.4. Therefore, by applying Theorems 2.2 and 2.3 from [13], the proof is complete.  $\square$

## 4.2 Stability of the Forward Map

This subsection contains the proof of Theorem 4.1. In Subsection 4.2.1 we study the case  $\beta = 1$ , where the forward map concerns an elliptic problem. Next, in Subsection 4.2.2 we establish the result for  $\beta > 1$ , where the forward map concerns a fractional elliptic problem. The proof for the fractional elliptic problem makes use of the result for the elliptic problem.

### 4.2.1 Elliptic Problem

The proof of Theorem 4.1 in the case  $\beta = 1$  follows a similar structure to that in [13], which shows stability of the forward map of an elliptic problem in Euclidean space. Some technical modifications are required to carry out the analysis in our metric graph setting.

*Proof of Theorem 4.1 for  $\beta = 1$ .* First, recall from Remark 3.5 that for  $\alpha > 1$  it holds almost surely that  $u \in H^{3/2}(\Gamma)$  for  $u \sim \mu_0$ . We will use this fact repeatedly without further notice. Let  $p := \mathcal{F}(u)$  be the solution to (3.1) with  $\beta = 1$  and input parameter  $u$ . Multiplying (3.1) by  $p$  and integrating gives

$$\int_{\Gamma} \kappa^2 p^2 \, dx - \int_{\Gamma} (\nabla \cdot (e^u \nabla p)) p \, dx = \int_{\Gamma} f p \, dx. \tag{4.14}$$

We rewrite the second term in the left-hand side of (4.14) in terms of the energy norm:

$$\int_{\Gamma} (\nabla \cdot (e^u \nabla p)) p \, dx = \sum_{e \in E} \int_e (\nabla \cdot (e^u \nabla p)) p \, dt$$

$$\begin{aligned}
&= - \sum_{e \in E} \int_e e^u |\nabla p|^2 dt + \sum_{v \in V} \sum_{e \in E_v} e^{u(v)} \partial_e p(v) p(v) \\
&= - \sum_{e \in E} \int_e e^u |\nabla p|^2 dt.
\end{aligned} \tag{4.15}$$

In the second line we have applied the divergence theorem on each edge, and the final equality follows from the Kirchhoff condition at every vertex, which forces the boundary flux terms to cancel. On the other hand, we can bound the right-hand side of (4.14) using Cauchy-Schwarz inequality:

$$\int_{\Gamma} f p dx \leq \|f\|_{L^2(\Gamma)} \|p\|_{H^1(\Gamma)}. \tag{4.16}$$

Combining (4.14), (4.15), and (4.16), we deduce that

$$\begin{aligned}
\min\{\kappa^2, e^{-\|u\|_{L^\infty(\Gamma)}}\} \|p\|_{H^1(\Gamma)}^2 &\leq \kappa^2 \|p\|_{L^2(\Gamma)}^2 + e^{-\|u\|_{L^\infty(\Gamma)}} \|\nabla p\|_{L^2(\Gamma)}^2 \\
&\leq \int_{\Gamma} f p dx \leq \|f\|_{L^2(\Gamma)} \|p\|_{H^1(\Gamma)},
\end{aligned}$$

which implies that

$$\|p\|_{H^1(\Gamma)} \leq \frac{1}{\min\{\kappa^2, e^{-\|u\|_{L^\infty(\Gamma)}}\}} \|f\|_{L^2(\Gamma)} \leq \frac{e^{\|u\|_{L^\infty(\Gamma)}}}{\min\{\kappa^2, 1\}} \|f\|_{L^2(\Gamma)} \leq C e^{\|u\|_{L^\infty(\Gamma)}} \|f\|_{L^2(\Gamma)}, \tag{4.17}$$

where  $C$  is a constant independent of  $u$ . This completes the proof of the bound (4.1) in the  $H^1(\Gamma)$  norm for  $\beta = 1$ . The bound in the  $L^\infty(\Gamma)$  norm then follows from Remark 4.2.

Next, we prove the bound (4.2). Let  $p_1 := \mathcal{F}(u_1)$  and  $p_2 := \mathcal{F}(u_2)$  be the solutions to (3.1) with  $\beta = 1$  and parameters  $u_1$  and  $u_2$ , respectively. By definition, it holds that

$$\begin{cases} \kappa^2 p_1 - \nabla \cdot (\exp(u_1) \nabla p_1) = f, \\ \kappa^2 p_2 - \nabla \cdot (\exp(u_2) \nabla p_2) = f. \end{cases}$$

Defining  $q := p_1 - p_2$  and subtracting the second equation from the first, we obtain

$$\kappa^2 q - \nabla \cdot (\exp(u_1) \nabla q) = \nabla \cdot ((\exp(u_1) - \exp(u_2)) \nabla p_2).$$

Multiplying both sides by  $q$  and integrating over  $\Gamma$ ,

$$\kappa^2 \int_{\Gamma} q^2 dx - \int_{\Gamma} \nabla \cdot (\exp(u_1) \nabla q) q dx = \int_{\Gamma} \nabla \cdot ((\exp(u_1) - \exp(u_2)) \nabla p_2) q dx.$$

Applying integration by parts to the left-hand side, along with the Kirchhoff vertex condition (3.1) of  $p_1$  and  $p_2$  guaranteed by Proposition 3.1, yields:

$$\kappa^2 \int_{\Gamma} q^2 dx + \int_{\Gamma} \exp(u_1) |\nabla q|^2 dx = \int_{\Gamma} \nabla \cdot ((\exp(u_1) - \exp(u_2)) \nabla p_2) q dx. \tag{4.18}$$

Now, since the assumption  $\alpha > 1$  ensures that  $u_1, u_2 \in L^\infty(\Gamma)$ , we can employ the Lipschitz continuity of the exponential function to estimate:

$$|\exp(u_1) - \exp(u_2)| \leq \|u_1 - u_2\|_{L^\infty(\Gamma)} \cdot \exp(\max\{\|u_1\|_{L^\infty(\Gamma)}, \|u_2\|_{L^\infty(\Gamma)}\}).$$

Using this bound, we deduce that

$$\begin{aligned}
\kappa^2 \|q\|_{L^2(\Gamma)}^2 + e^{-\|u_1\|_{L^\infty(\Gamma)}} \|\nabla q\|_{L^2(\Gamma)}^2 &\leq \kappa^2 \int_{\Gamma} q^2 \, dx + \int_{\Gamma} \exp(u_1) |\nabla q|^2 \, dx \\
&\leq \left| \int_{\Gamma} \nabla \cdot \left( (\exp(u_1) - \exp(u_2)) \nabla p_2 \right) q \, dx \right| = \left| \int_{\Gamma} (\exp(u_1) - \exp(u_2)) \nabla p_2 \cdot \nabla q \, dx \right| \\
&\leq \exp\left(\max\{\|u_1\|_{L^\infty(\Gamma)}, \|u_2\|_{L^\infty(\Gamma)}\}\right) \|u_1 - u_2\|_{L^\infty(\Gamma)} \|\nabla p_2\|_{L^2(\Gamma)} \|\nabla q\|_{L^2(\Gamma)} \\
&\leq \frac{1}{2} \exp(\|u_1\|_{L^\infty(\Gamma)}) \exp\left(2 \max\{\|u_1\|_{L^\infty(\Gamma)}, \|u_2\|_{L^\infty(\Gamma)}\}\right) \|u_1 - u_2\|_{L^\infty(\Gamma)}^2 \|\nabla p_2\|_{L^2(\Gamma)}^2 \\
&\quad + \frac{1}{2} \exp(-\|u_1\|_{L^\infty(\Gamma)}) \|\nabla q\|_{L^2(\Gamma)}^2, \\
&\leq \frac{1}{2} \exp\left(3 \max\{\|u_1\|_{L^\infty(\Gamma)}, \|u_2\|_{L^\infty(\Gamma)}\}\right) \|u_1 - u_2\|_{L^\infty(\Gamma)}^2 \|\nabla p_2\|_{L^2(\Gamma)}^2 + \frac{1}{2} e^{-\|u_1\|_{L^\infty(\Gamma)}} \|\nabla q\|_{L^2(\Gamma)}^2,
\end{aligned}$$

where in the second-to-last step we used Young's inequality  $ab \leq \frac{1}{2\varepsilon}a^2 + \frac{\varepsilon}{2}b^2$  with  $a = \exp\left(\max\{\|u_1\|_{L^\infty(\Gamma)}, \|u_2\|_{L^\infty(\Gamma)}\}\right) \|u_1 - u_2\|_{L^\infty(\Gamma)} \|\nabla p_2\|_{L^2(\Gamma)}$ ,  $b = \|\nabla q\|_{L^2(\Gamma)}$ , and  $\varepsilon = e^{-\|u_1\|_{L^\infty(\Gamma)}}$ . Therefore, since  $\|q\|_{H^1(\Gamma)}^2 = \|q\|_{L^2(\Gamma)}^2 + \|\nabla q\|_{L^2(\Gamma)}^2$ , we obtain that

$$\begin{aligned}
&\|q\|_{H^1(\Gamma)}^2 \\
&\leq \frac{1}{2 \min\{\kappa^2, \frac{1}{2}e^{-\|u_1\|_{L^\infty(\Gamma)}}\}} \exp\left(3 \max\{\|u_1\|_{L^\infty(\Gamma)}, \|u_2\|_{L^\infty(\Gamma)}\}\right) \|u_1 - u_2\|_{L^\infty(\Gamma)}^2 \|\nabla p_2\|_{L^2(\Gamma)}^2 \\
&\leq \frac{e^{\|u_1\|_{L^\infty(\Gamma)}}}{\min\{2\kappa^2, 1\}} \exp\left(3 \max\{\|u_1\|_{L^\infty(\Gamma)}, \|u_2\|_{L^\infty(\Gamma)}\}\right) \|u_1 - u_2\|_{L^\infty(\Gamma)}^2 \|\nabla p_2\|_{L^2(\Gamma)}^2 \\
&\leq \frac{1}{\min\{2\kappa^2, 1\}} \exp\left(4 \max\{\|u_1\|_{L^\infty(\Gamma)}, \|u_2\|_{L^\infty(\Gamma)}\}\right) \|u_1 - u_2\|_{L^\infty(\Gamma)}^2 \|\nabla p_2\|_{L^2(\Gamma)}^2.
\end{aligned}$$

Finally, applying the estimate from (4.17) to control  $\|\nabla p_2\|_{L^2(\Gamma)}$  in terms of  $\|f\|_{L^2(\Gamma)}$  and  $\|u_2\|_{L^\infty(\Gamma)}$ , we conclude that

$$\|q\|_{H^1(\Gamma)} \leq C \|f\|_{L^2(\Gamma)} \exp\left(3 \max\{\|u_1\|_{L^\infty(\Gamma)}, \|u_2\|_{L^\infty(\Gamma)}\}\right) \|u_1 - u_2\|_{L^\infty(\Gamma)},$$

for a constant  $C > 0$  that depends only on  $\kappa$  and  $\Gamma$ . We have hence established the bound (4.2) in the  $H^1(\Gamma)$  norm. The bound in the  $L^\infty(\Gamma)$  norm then follows from Remark 4.2, concluding the proof of Theorem 4.1 for  $\beta = 1$ .  $\square$

#### 4.2.2 Fractional Elliptic Problem

Here, we prove Theorem 4.1 in the case  $\beta > 1$ . The proof technique that we used in the case  $\beta = 1$ —based on a weak formulation—cannot be applied directly, since now  $\mathcal{L}_u^\beta$  is defined spectrally. Instead, we will leverage a series representation of the solution, along with Weyl's law for  $\mathcal{L}_u$  and the stability of the elliptic forward map proved in the previous subsection.

We first introduce a new version of the Weyl's law on metric graphs established in [3], in which we ensure that the constants are independent of the input parameter  $u$ .

**Lemma 4.6.** *Let  $\mathcal{L}_u$  be the second-order elliptic operator defined in (3.1) with  $u \in H^{3/2}(\Gamma)$ . Then, there exist constants  $C_1, C_2 > 0$  independent of  $u$  such that, for all  $j \in \mathbb{N}$ ,*

$$C_1 \exp(-\|u\|_{L^\infty(\Gamma)}) j^2 \leq \lambda_j \leq C_2 \exp(\|u\|_{L^\infty(\Gamma)}) j^2,$$

where  $\{\lambda_j\}_{j \in \mathbb{N}}$  are the eigenvalues of  $\mathcal{L}_u$  arranged in non-decreasing order.

*Proof.* To clarify the dependence of the constants on  $u$  using the classical Weyl's law [30], we denote  $M := \|u\|_{L^\infty(\Gamma)}$  and consider two constant-coefficient elliptic operators as extreme cases:

$$\begin{cases} \mathcal{L}_{-M} := -\nabla \cdot (e^{-M} \nabla \cdot) + \kappa^2 = \kappa^2 - e^{-M} \Delta, \\ \mathcal{L}_{+M} := -\nabla \cdot (e^M \nabla \cdot) + \kappa^2 = \kappa^2 - e^M \Delta, \end{cases}$$

each equipped with the same Kirchhoff vertex conditions as  $\mathcal{L}_u$ . For any non-zero  $v \in H^1(\Gamma)$ , introduce the Rayleigh quotients (see [12], pp. 401-405)

$$\begin{cases} \mathcal{R}_{-M}(v) = \frac{\int_{\Gamma} e^{-M} |v'|^2 dx + \kappa^2 \int_{\Gamma} |v|^2 dx}{\|v\|_{L^2(\Gamma)}^2}, \\ \mathcal{R}_u(v) = \frac{\int_{\Gamma} e^u |v'|^2 dx + \kappa^2 \int_{\Gamma} |v|^2 dx}{\|v\|_{L^2(\Gamma)}^2}, \\ \mathcal{R}_{+M}(v) = \frac{\int_{\Gamma} e^M |v'|^2 dx + \kappa^2 \int_{\Gamma} |v|^2 dx}{\|v\|_{L^2(\Gamma)}^2}. \end{cases}$$

Since  $e^{-M} \leq e^u \leq e^M$  on  $\Gamma$ , it follows that

$$\mathcal{R}_{-M}(v) \leq \mathcal{R}_u(v) \leq \mathcal{R}_{+M}(v), \quad \forall v \in H^1(\Gamma) \setminus \{0\}.$$

The paper [3] establishes that  $\mathcal{L}_u$  is self-adjoint with compact inverse on the compact, locally one-dimensional graph  $\Gamma$ . Hence, the Courant–Fischer (min–max) characterization (see [12], pp. 405–408) applies verbatim as in the classical Euclidean or manifold setting. Applying the Courant–Fischer min–max principle, we have

$$\lambda_j(\mathcal{L}_{-M}) = \min_{\substack{V \subset H^1(\Gamma) \\ \dim V = j}} \max_{v \in V} \mathcal{R}_{-M}(v) \leq \lambda_j(\mathcal{L}_u) \leq \min_{\substack{V \subset H^1(\Gamma) \\ \dim V = j}} \max_{v \in V} \mathcal{R}_{+M}(v) = \lambda_j(\mathcal{L}_{+M}). \quad (4.19)$$

Classical Weyl's law [30] for the constant-coefficient operator  $\mathcal{L} = -\Delta$  (with Kirchhoff vertex conditions) on a compact metric graph gives constants  $C'_1, C'_2 > 0$  (depending only on  $\Gamma$ ) such that

$$C'_1 j^2 \leq \lambda_j(\mathcal{L}) \leq C'_2 j^2.$$

Hence

$$C'_1 e^{-M} j^2 \leq \lambda_j(\mathcal{L}_{-M}), \quad \lambda_j(\mathcal{L}_{+M}) \leq C'_2 e^M j^2. \quad (4.20)$$

Combining (4.20) with (4.19) yields

$$C_1 e^{-\|u\|_{L^\infty(\Gamma)}} j^2 \leq \lambda_j(\mathcal{L}_u) \leq C_2 e^{\|u\|_{L^\infty(\Gamma)}} j^2,$$

where  $C_1$  and  $C_2$  depend only on  $\Gamma$  and  $\kappa$ . □

Lemma 4.6 can be used to establish the following lemma, which controls the difference between powers of the eigenvalues of  $\mathcal{L}_{u_1}$  and  $\mathcal{L}_{u_2}$ , for given  $u_1, u_2 \in H^{3/2}(\Gamma)$ , in terms of the  $L^\infty(\Gamma)$  deviation between  $u_1$  and  $u_2$ .

**Lemma 4.7.** *Let  $\mathcal{L}_{u_1}$  and  $\mathcal{L}_{u_2}$  be defined as in (3.1) with  $u_1, u_2 \in H^{3/2}(\Gamma)$ . Then, there exists a constant  $C > 0$  independent of  $u_1, u_2$  such that, for  $s \geq 0$ ,*

$$|(\lambda_j^{(1)})^{-s} - (\lambda_j^{(2)})^{-s}| \leq C \exp\left((s+2) \max\{\|u_1\|_{L^\infty(\Gamma)}, \|u_2\|_{L^\infty(\Gamma)}\}\right) \|u_1 - u_2\|_{L^\infty(\Gamma)},$$

where  $\{\lambda_j^{(i)}\}_{j \in \mathbb{N}}$  are the eigenvalues of  $\mathcal{L}_{u_i}$  arranged in non-decreasing order,  $(i = 1, 2)$ .

*Proof.* We first estimate  $|\lambda_j^{(1)} - \lambda_j^{(2)}|$ . Setting the Rayleigh quotient (see [12], pp. 401–404) of  $\mathcal{L}_{u_i}$ ,  $(i = 1, 2)$  to be the following form

$$\mathcal{R}_{u_i}(v) = \frac{\int_{\Gamma} e^{u_i} |v'|^2 dx + \kappa^2 \int_{\Gamma} |v|^2 dx}{\|v\|_{L^2(\Gamma)}^2}, \quad (i = 1, 2)$$

then by the Courant–Fischer min–max principle (see [12], pp. 405–408), it holds that

$$\lambda_j^{(i)} = \min_{\substack{V \subset H^1(\Gamma) \\ \dim V = j}} \max_{0 \neq v \in V} \mathcal{R}_{u_i}(v).$$

Hence, the eigenvalues can be expressed in the min-max form

$$\lambda_j^{(1)} = \min_{\substack{V \subset H^1(\Gamma) \\ \dim V = j}} \max_{0 \neq v \in V} \mathcal{R}_{u_1}(v), \quad \lambda_j^{(2)} = \min_{\substack{V \subset H^1(\Gamma) \\ \dim V = j}} \max_{0 \neq v \in V} \mathcal{R}_{u_2}(v).$$

Let  $V_2$  be a  $j$ -dimensional subspace realizing the minimum for  $\lambda_j^{(2)}$ . Then,

$$\lambda_j^{(1)} - \lambda_j^{(2)} \leq \max_{0 \neq v \in V_2} \mathcal{R}_{u_1}(v) - \max_{0 \neq v \in V_2} \mathcal{R}_{u_2}(v) \leq \max_{0 \neq v \in V_2} |\mathcal{R}_{u_1}(v) - \mathcal{R}_{u_2}(v)|.$$

Similarly, letting  $V_1$  realize the minimum for  $\lambda_j^{(1)}$  gives

$$\lambda_j^{(2)} - \lambda_j^{(1)} \leq \max_{0 \neq v \in V_1} |\mathcal{R}_{u_1}(v) - \mathcal{R}_{u_2}(v)|.$$

Combining these two estimates yields

$$|\lambda_j^{(1)} - \lambda_j^{(2)}| \leq \max\left\{\max_{0 \neq v \in V_1}, \max_{0 \neq v \in V_2}\right\} |\mathcal{R}_{u_1}(v) - \mathcal{R}_{u_2}(v)| \leq \sup_{0 \neq v \in H^1(\Gamma)} |\mathcal{R}_{u_1}(v) - \mathcal{R}_{u_2}(v)|.$$

Notice that, for any  $v \neq 0$ ,

$$\begin{aligned} |\mathcal{R}_{u_1}(v) - \mathcal{R}_{u_2}(v)| &= \frac{\left| \int_{\Gamma} (e^{u_1} - e^{u_2}) |v'|^2 dx \right|}{\|v\|_{L^2(\Gamma)}^2} \\ &\leq \|e^{u_1} - e^{u_2}\|_{L^\infty(\Gamma)} \frac{\|v'\|_{L^2(\Gamma)}^2}{\|v\|_{L^2(\Gamma)}^2} \leq e^M \|u_1 - u_2\|_{L^\infty(\Gamma)} \frac{\|v'\|_{L^2(\Gamma)}^2}{\|v\|_{L^2(\Gamma)}^2}, \end{aligned} \quad (4.21)$$

where  $M := \max\{\|u_1\|_{L^\infty(\Gamma)}, \|u_2\|_{L^\infty(\Gamma)}\}$ . Taking the infimum over all  $j$ -dimensional subspaces in the last ratio gives the  $j$ th eigenvalue of  $-\Delta$  with Kirchhoff conditions. By the classical Weyl's law on the compact metric graph (see [30]), there exists a constant  $c(\Gamma)$ , independent of  $u$ , such that  $\lambda_j(-\Delta) \leq c(\Gamma) j^2$ , for all  $j \in \mathbb{N}$ . Thus, (4.21) implies that

$$|\lambda_j^{(1)} - \lambda_j^{(2)}| \leq e^M \|u_1 - u_2\|_{L^\infty(\Gamma)} \lambda_j(-\Delta) \leq c(\Gamma) e^M j^2 \|u_1 - u_2\|_{L^\infty(\Gamma)}.$$



For general  $s \geq 0$ , the mean-value theorem applied to  $x \mapsto x^{-s}$  yields

$$|(\lambda_j^{(1)})^{-s} - (\lambda_j^{(2)})^{-s}| = s \xi_j^{-s-1} |\lambda_j^{(1)} - \lambda_j^{(2)}|,$$

where  $\xi_j$  lies between  $\lambda_j^{(1)}$  and  $\lambda_j^{(2)}$ . Using  $\xi_j^{-s-1} \leq C e^{(s+1)M} j^{-2(s+1)}$  from Lemma 4.6, in which  $C$  is independent of  $u$  and the above  $O(j^2)$  bound, we obtain

$$\begin{aligned} |(\lambda_j^{(1)})^{-s} - (\lambda_j^{(2)})^{-s}| &\leq C e^{(s+2)M} j^{-2s} \|u_1 - u_2\|_{L^\infty(\Gamma)} \\ &\leq C \exp\left((s+2) \max\{\|u_1\|_{L^\infty(\Gamma)}, \|u_2\|_{L^\infty(\Gamma)}\}\right) \|u_1 - u_2\|_{L^\infty(\Gamma)}, \end{aligned}$$

since  $j^{-2s} \leq 1$  for  $j \geq 1$  and  $s \geq 0$ . This completes the proof.  $\square$

We are now ready to prove the stability of the forward map for the fractional elliptic problem.

*Proof of Theorem 4.1 for  $\beta > 1$ .* For  $\beta > 1$ , since the operator is defined in the spectral sense, we cannot directly apply the weak formulation used in the proof for the case  $\beta = 1$ . Instead, we begin with the series representation of the solution:

$$p = \sum_{j=1}^{\infty} f_j \lambda_j^{-\beta} e_j, \quad (4.22)$$

where  $\{\lambda_j\}$  are the non-decreasingly ordered eigenvalues of  $\mathcal{L}_u$ ,  $f_j = \langle f, e_j \rangle_{L^2(\Gamma)}$ , and  $\{e_j\}$  are the corresponding  $L^2(\Gamma)$ -normalized eigenfunctions.

For the case  $\beta = 1$ , we have already established that there exists  $C_0 > 0$  independent of  $u$ , such that the solution  $p_1$  satisfies:

$$\|p_1\|_{L^2(\Gamma)}^2 = \sum_{j=1}^{\infty} |f_j \lambda_j^{-1}|^2 < C_0 \exp(2\|u\|_{L^\infty(\Gamma)}).$$

We now estimate  $\|p\|_{L^2(\Gamma)}$  for the general case  $\beta > 1$ :

$$\begin{aligned} \|p\|_{L^2(\Gamma)}^2 &= \sum_{j=1}^{\infty} |f_j \lambda_j^{-\beta}|^2 = \sum_{j=1}^{\infty} |f_j|^2 \cdot \lambda_j^{-2\beta} \\ &\stackrel{(i)}{\leq} C_0 \exp(2\beta\|u\|_{L^\infty(\Gamma)}) \cdot \sum_{j=1}^{\infty} |f_j|^2 j^{-4\beta} \leq c_0(\beta) \exp(2\beta\|u\|_{L^\infty(\Gamma)}), \end{aligned} \quad (4.23)$$

where inequality (i) follows from Lemma 4.6, and  $c_0(\beta)$  is a decreasing function of  $\beta$ .

Next, we analyze  $\|\nabla p\|_{L^2(\Gamma)}$ . We begin with the eigenfunctions  $\{e_j\}$ . By the definition of the eigenfunction  $e_j$ , we have

$$(\kappa^2 - \nabla \cdot (\exp(u) \nabla \cdot)) e_j = \lambda_j e_j.$$

Taking the inner product with  $e_j$  in  $L^2(\Gamma)$  and applying integration by parts and using that the eigenfunctions are in the domain of the operator, and thus satisfy the Kirchhoff vertex conditions, we obtain

$$\int_{\Gamma} \kappa^2 e_j^2 \, dx + \int_{\Gamma} \exp(u) |\nabla e_j|^2 \, dx = \lambda_j \int_{\Gamma} e_j^2 \, dx.$$

Using the normalization condition  $\|e_j\|_{L^2(\Gamma)} = 1$ , it follows that

$$\int_{\Gamma} \exp(u) |\nabla e_j|^2 \, dx = \lambda_j - \kappa^2.$$

Since  $u \in L^\infty(\Gamma)$ , we deduce that

$$\exp(-\|u\|_{L^\infty(\Gamma)}) \|\nabla e_j\|_{L^2(\Gamma)}^2 \leq \lambda_j - \kappa^2 \leq \exp(\|u\|_{L^\infty(\Gamma)}) \|\nabla e_j\|_{L^2(\Gamma)}^2.$$

Consequently,

$$\exp(-\|u\|_{L^\infty(\Gamma)}) (\lambda_j - \kappa^2) \leq \|\nabla e_j\|_{L^2(\Gamma)}^2 \leq \exp(\|u\|_{L^\infty(\Gamma)}) (\lambda_j - \kappa^2),$$

implying that there exist constants  $C_1, C_2 > 0$ , independent of  $u$ , such that

$$C_1 \exp\left(-\frac{1}{2}\|u\|_{L^\infty(\Gamma)}\right) \lambda_j^{1/2} \leq \|\nabla e_j\|_{L^2(\Gamma)} \leq C_2 \exp\left(\frac{1}{2}\|u\|_{L^\infty(\Gamma)}\right) \lambda_j^{1/2}. \quad (4.24)$$

Noting that  $\Gamma$  is a compact metric graph, term-by-term differentiation of the series is justified due to uniform convergence. We estimate  $\|\nabla p\|_{L^2(\Gamma)}$  as follows:

$$\begin{aligned} \|\nabla p\|_{L^2(\Gamma)} &= \left\| \sum_{j=1}^{\infty} f_j \lambda_j^{-\beta} \nabla e_j \right\|_{L^2(\Gamma)} \leq \sum_{j=1}^{\infty} |f_j| \lambda_j^{-\beta} \|\nabla e_j\|_{L^2(\Gamma)} \\ &\stackrel{(ii)}{\leq} C_2 \exp\left(\frac{1}{2}\|u\|_{L^\infty(\Gamma)}\right) \sum_{j=1}^{\infty} |f_j| \lambda_j^{-\beta} \lambda_j^{1/2} = C_2 \exp\left(\frac{1}{2}\|u\|_{L^\infty(\Gamma)}\right) \sum_{j=1}^{\infty} |f_j| \lambda_j^{-(\beta-\frac{1}{2})} \\ &\stackrel{(iii)}{\leq} C_3 \exp\left(\left(\beta - \frac{1}{2} + \frac{1}{2}\right)\|u\|_{L^\infty(\Gamma)}\right) \sum_{j=1}^{\infty} |f_j|^2 j^{-(\beta-\frac{1}{2})} \\ &\leq c_1(\beta) \exp(\beta\|u\|_{L^\infty(\Gamma)}). \end{aligned} \quad (4.25)$$

Here, we obtained inequality (ii) by using (4.24), and inequality (iii) follows directly since by assumption  $f \in L^2(\Gamma)$ . Combining estimates (4.23) and (4.25), we obtain a bound for the  $H^1(\Gamma)$  norm of  $p$  when  $\beta > 1$ :

$$\|p\|_{H^1(\Gamma)} \leq c(\beta) \exp(\beta\|u\|_{L^\infty(\Gamma)}), \quad (4.26)$$

where  $c(\beta)$  is independent of  $u$  and a decreasing function of  $\beta$ .

We now derive an estimate for  $\|p_1 - p_2\|_{H^1(\Gamma)}$ . Employing the series representation of the solutions  $p_1$  and  $p_2$ , we express their difference as

$$\begin{aligned} \tilde{p} := p_1 - p_2 &= \sum_{j=1}^{\infty} f_j^{(1)} (\lambda_j^{(1)})^{-\beta} e_j^{(1)} - \sum_{j=1}^{\infty} f_j^{(2)} (\lambda_j^{(2)})^{-\beta} e_j^{(2)} \\ &= \sum_{j=1}^{\infty} \left[ f_j^{(1)} (\lambda_j^{(1)})^{-\beta} e_j^{(1)} - f_j^{(2)} (\lambda_j^{(2)})^{-\beta} e_j^{(2)} \right] \\ &= \sum_{j=1}^{\infty} \left[ (\lambda_j^{(1)})^{-(\beta-1)} f_j^{(1)} (\lambda_j^{(1)})^{-1} e_j^{(1)} - (\lambda_j^{(2)})^{-(\beta-1)} f_j^{(2)} (\lambda_j^{(2)})^{-1} e_j^{(2)} \right], \end{aligned}$$

where  $\{(\lambda_j^{(1)}, e_j^{(1)})\}_{j \in \mathbb{N}}$  and  $\{(\lambda_j^{(2)}, e_j^{(2)})\}_{j \in \mathbb{N}}$  represent the eigenpairs of the operators  $\mathcal{L}_{u_1}$  and  $\mathcal{L}_{u_2}$  with standard Kirchhoff vertex conditions, ordered and normalized in the standard way.

We first estimate  $\|p_1 - p_2\|_{L^2(\Gamma)}$ . Since the eigenfunctions for different operators  $\mathcal{L}_{u_1}$  and  $\mathcal{L}_{u_2}$  are no longer orthogonal, we will need to employ the results for  $\beta = 1$ , as well as Lemmas 4.6 and 4.7. As shown in [3],  $\mathcal{L}_{u_1}$  is self-adjoint, positive definite with compact inverse in  $L^2(\Gamma)$ . Hence, the spectral theorem yields that for  $\beta > 1$ ,  $\mathcal{L}_{u_1}^{-(\beta-1)}$  is again self-adjoint, positive definite, and compact, with discrete spectrum. Thus, we can estimate the operator norm of  $\mathcal{L}_{u_1}^{-(\beta-1)}$  by using Lemma 4.6,

$$\|\mathcal{L}_{u_1}^{-(\beta-1)}\|_{op} = \sup_j (\lambda_j^{(1)})^{-(\beta-1)} = (\lambda_1^{(1)})^{-(\beta-1)} \leq C \exp(-(\beta-1)\|u_1\|_{L^\infty(\Gamma)}), \quad (4.27)$$

where  $C$  is a constant independent of  $u_1$ . Therefore,

$$\begin{aligned}
\|p_1 - p_2\|_{L^2(\Gamma)} &= \left\| \sum_{j=1}^{\infty} (\lambda_j^{(1)})^{-(\beta-1)} f_j^{(1)} (\lambda_j^{(1)})^{-1} e_j^{(1)} - (\lambda_j^{(2)})^{-(\beta-1)} f_j^{(2)} (\lambda_j^{(2)})^{-1} e_j^{(2)} \right\|_{L^2(\Gamma)} \\
&\leq \left\| \sum_{j=1}^{\infty} (\lambda_j^{(1)})^{-(\beta-1)} [f_j^{(1)} (\lambda_j^{(1)})^{-1} e_j^{(1)} - f_j^{(2)} (\lambda_j^{(2)})^{-1} e_j^{(2)}] \right\|_{L^2(\Gamma)} \\
&\quad + \left\| \sum_{j=1}^{\infty} [(\lambda_j^{(1)})^{-(\beta-1)} - (\lambda_j^{(2)})^{-(\beta-1)}] f_j^{(2)} (\lambda_j^{(2)})^{-1} e_j^{(2)} \right\|_{L^2(\Gamma)} \\
&\stackrel{(iv)}{\leq} \|\mathcal{L}_{u_1}^{-(\beta-1)}\|_{\text{op}} \|p_1^{(1)} - p_2^{(1)}\|_{L^2(\Gamma)} \\
&\quad + \left\| \sum_{j=1}^{\infty} [(\lambda_j^{(1)})^{-(\beta-1)} - (\lambda_j^{(2)})^{-(\beta-1)}] f_j^{(2)} (\lambda_j^{(2)})^{-1} e_j^{(2)} \right\|_{L^2(\Gamma)} \\
&\stackrel{(v)}{\leq} c_2(\beta) \exp((\beta-1)\|u_1\|_{L^\infty(\Gamma)}) \|p_1^{(1)} - p_2^{(1)}\|_{L^2(\Gamma)} \\
&\quad + c_3(\beta) \exp((\beta+1) \max\{\|u_1\|_{L^\infty(\Gamma)}, \|u_2\|_{L^\infty(\Gamma)}\}) \|p_2^{(1)}\|_{L^2(\Gamma)} \\
&\stackrel{(vi)}{\leq} c_4(\beta) \exp((\beta+2) \max\{\|u_1\|_{L^\infty(\Gamma)}, \|u_2\|_{L^\infty(\Gamma)}\}) \|u_1 - u_2\|_{L^\infty(\Gamma)}, \quad (4.28)
\end{aligned}$$

where  $p_1^{(1)}$  and  $p_2^{(1)}$  denote the solutions of (3.1) with  $\beta = 1$  and parameters  $u_1$  and  $u_2$ , respectively. In inequality (iv) we invoke the operator-norm estimate (4.27). Inequality (v) relies on Lemmas 4.6 and 4.7, while inequality (vi) is obtained by applying Theorem 4.1 with  $\beta = 1$ .

Next, we estimate  $\|\nabla p_1 - \nabla p_2\|_{L^2(\Gamma)}$ . Proceeding analogously, we have

$$\begin{aligned}
\|\nabla p_1 - \nabla p_2\|_{L^2(\Gamma)} &= \left\| \sum_{j=1}^{\infty} (\lambda_j^{(1)})^{-(\beta-1)} f_j^{(1)} (\lambda_j^{(1)})^{-1} \nabla e_j^{(1)} - (\lambda_j^{(2)})^{-(\beta-1)} f_j^{(2)} (\lambda_j^{(2)})^{-1} \nabla e_j^{(2)} \right\|_{L^2(\Gamma)} \\
&\leq \left\| \sum_{j=1}^{\infty} (\lambda_j^{(1)})^{-(\beta-1)} [f_j^{(1)} (\lambda_j^{(1)})^{-1} \nabla e_j^{(1)} - f_j^{(2)} (\lambda_j^{(2)})^{-1} \nabla e_j^{(2)}] \right\|_{L^2(\Gamma)} \\
&\quad + \left\| \sum_{j=1}^{\infty} [(\lambda_j^{(1)})^{-(\beta-1)} - (\lambda_j^{(2)})^{-(\beta-1)}] f_j^{(2)} (\lambda_j^{(2)})^{-1} \nabla e_j^{(2)} \right\|_{L^2(\Gamma)} \\
&\stackrel{(vii)}{\leq} \max_j (\lambda_j^{(1)})^{-(\beta-1)} \left\| \sum_{j=1}^{\infty} [f_j^{(1)} (\lambda_j^{(1)})^{-1} \nabla e_j^{(1)} - f_j^{(2)} (\lambda_j^{(2)})^{-1} \nabla e_j^{(2)}] \right\|_{L^2(\Gamma)} \\
&\quad + \left\| \sum_{j=1}^{\infty} [(\lambda_j^{(1)})^{-(\beta-1)} - (\lambda_j^{(2)})^{-(\beta-1)}] f_j^{(2)} (\lambda_j^{(2)})^{-1} \nabla e_j^{(2)} \right\|_{L^2(\Gamma)} \\
&\leq c_2(\beta) \exp((\beta-1)\|u_1\|_{L^\infty(\Gamma)}) \|\nabla p_1^{(1)} - \nabla p_2^{(1)}\|_{L^2(\Gamma)} \\
&\quad + c_3(\beta) \exp((\beta+1)\|u_1\|_{L^\infty(\Gamma)}) \|u_1 - u_2\|_{L^\infty(\Gamma)} \|\nabla p_2\|_{L^2(\Gamma)} \\
&\stackrel{(viii)}{\leq} c_4(\beta) \exp((\beta+2)\|u_1\|_{L^\infty(\Gamma)}) \|u_1 - u_2\|_{L^\infty(\Gamma)}, \quad (4.29)
\end{aligned}$$

where in (vii) we used Lemmas 4.6 and 4.7, and (viii) follows from Theorem 4.1 with  $\beta = 1$ , proved in Subsection 4.2.1. Combining the estimates in (4.28) and (4.29), we deduce that

$$\|p_1 - p_2\|_{H^1(\Gamma)} \leq c(\beta) \exp((\beta+2)\|u_1\|_{L^\infty(\Gamma)}) \|u_1 - u_2\|_{L^\infty(\Gamma)},$$

as desired.  $\square$

## 5 Numerical Experiments

In this section, we illustrate the numerical solution of elliptic and fractional elliptic Bayesian inverse problems on compact metric graphs. Subsection 5.1 details the algorithmic implementation, while Subsections 5.2 and 5.3 present numerical results for the elliptic and fractional elliptic problems, respectively. We compare the accuracy of *maximum a posteriori* (MAP) and posterior mean estimators; see e.g. [32] for their definitions. In addition, we explore the quantification of uncertainty through the posterior marginal standard deviation along points in the graph.

### 5.1 Implementation

We work on a letter-shaped metric graph naturally embedded in  $\mathbb{R}^2$  (see e.g. Figure 1) and adopt the Bayesian framework introduced in Section 3. For the forward map induced by Equation 3.1, we set  $\kappa = 1$  and  $f(x) = z_1^2(x) - z_2^2(x)$ , where  $(z_1(x), z_2(x))$  denotes the Cartesian coordinates of the point  $x \in \Gamma \subset \mathbb{R}^2$ . We examine both the standard elliptic case with  $\beta = 1$  (Subsection 5.2) and the fractional elliptic case with  $\beta = 3/2$  (Subsection 5.3). The prior for  $u$  is a Whittle–Matérn Gaussian field as specified in Equation 3.6, with smoothness parameter  $\alpha = 1$ , where the validity of this choice is guaranteed by Remark 3.5. We further take  $\kappa_0 = \sqrt{0.2} \cdot 2/3$  and  $a = 0.2$ , which leads to a correlation range of 3 in the setting of the `MetricGraph` R package [8].

We discretize the letter-shaped metric graph in a fine mesh and approximate the forward model and the prior using the finite-element method introduced in [2] and implemented in the `rSPDE` [7] and `MetricGraph` [8] R packages. As we choose  $\alpha = 1$ , the random field  $u$  can be simulated exactly through the methods in [6]; however, as we discretize the forward problem, we also use a finite-element approximation of  $u$  as introduced in [3] and further refined in [4]. To balance accuracy and computational efficiency, we use a mesh size of  $h = 0.05$  for the elliptic problem and  $h = 0.2$  for the fractional case, thus reducing the computational cost in the fractional case. For the latter case, we employ the operator-based approach from [2].

The number of mesh points for the elliptic and fractional elliptic problems are 1,998 and 507, respectively. In each case, we draw a (discretized) ground-truth parameter  $u_0$  from the prior and obtain point-wise observations by evaluating the numerically computed ground-truth solution  $p_0$  at all mesh points, and adding a spatially-varying observation noise term. Specifically, at each mesh point, we set

$$y_i = p_0[i] + (\mathbf{n}_{\text{rel}} |p_0[i]| + \mathbf{n}_{\text{abs}}) \varepsilon_i, \quad \varepsilon_i \stackrel{\text{i.i.d.}}{\sim} \mathcal{N}(0, 1),$$

where  $\mathbf{n}_{\text{rel}} = 0.05$  controls the relative noise level and  $\mathbf{n}_{\text{abs}} = 0.10$  ensures a nonnegligible noise floor even when  $p_0[i]$  is small. This mixed noise model yields meaningful uncertainty at both large and small scales, and helps avoid the ill-conditioning of the likelihood that would emerge when using a single fixed noise level over the wide range of values of  $p_0$ .

For posterior sampling, we use the preconditioned Crank–Nicolson (pCN) MCMC method [11], which preserves the Gaussian prior in the proposal and reduces the Metropolis–Hastings ratio to the posterior-to-prior term alone, thereby avoiding explicit covariance inversions. The discretization-independent rate of convergence (uniform spectral gap) of pCN was established in [20]; see also [16] for a study of pCN on (non-metric) graphs. Here, we further incorporate a simple self-adaptive update for the step size  $\tau$  to balance acceptance and exploration, and apply temperature annealing to accelerate convergence of the chain; we refer to [31, Chapter 7] for an introduction to annealing strategies for Monte Carlo methods. The procedure is outlined in Algorithm 5.1 below.

---

**Algorithm 5.1** Adaptive pCN MCMC with Temperature Annealing

---

**Require:** Prior  $\mu_0$ , data  $y$  and potential function  $\Phi(\cdot; y)$ , initial step size  $\tau$ , minimum step size  $\tau_{\min}$ , annealing start  $T_0$ , cooling factor  $\zeta$ , sample size  $N$ , adaptation interval  $N_{\text{adapt}}$ , target acceptance rate  $r_{\text{target}}$ , burn-in  $B$ .

- 1: **Initialization:** Sample  $u^{(0)} \sim \mu_0$ .
- 2: **for**  $n = 1, \dots, N$  **do**
- 3:   **Proposal step:** Set
$$v := \sqrt{1 - \tau^2} u^{(n-1)} + \tau \xi, \quad \xi \sim \mu_0.$$
- 4:   **Accept/reject step:** Set temperature  $T_n := \max(1, T_0 \zeta^{\lfloor n/N_{\text{adapt}} \rfloor})$ , and set

$$u^{(n)} := \begin{cases} v, & \text{with probability } \min\left\{1, \exp\left(\frac{\Phi(u^{(n-1)}; y) - \Phi(v; y)}{T_n}\right)\right\}, \\ u^{(n-1)}, & \text{with probability } 1 - \min\left\{1, \exp\left(\frac{\Phi(u^{(n-1)}; y) - \Phi(v; y)}{T_n}\right)\right\}. \end{cases}$$

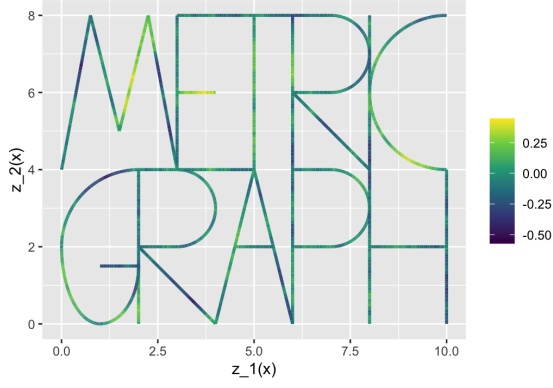
- 5:   Record acceptance indicator.
  - 6:   **if**  $n \bmod N_{\text{adapt}} = 0$  **then**
  - 7:     Compute recent acceptance rate  $\bar{r}$ .
  - 8:     **if**  $\bar{r} < 0.9 r_{\text{target}}$  **then**  $\tau \leftarrow \max(0.9 \tau, \tau_{\min})$ .
  - 9:     **else if**  $\bar{r} > 1.1 r_{\text{target}}$  **then**  $\tau \leftarrow 1.2 \tau$ .
  - 10:    **end if**
  - 11:   **end if**
  - 12: **end for**
  - 13: **return**  $\{u^{(n)}\}_{n=B+1}^N$  (discard first  $B$  burn-in samples) and acceptance history.
- 

In the experiments described in the following subsections, we carefully select hyperparameters such as  $N$ ,  $\tau$ , and  $\tau_{\min}$  to balance exploration and acceptance rate. We use a sample size  $N = 10^5$  in both Subsections 5.2 and 5.3. For the initial step size, we choose  $\tau = 0.3$ , with a minimum step size  $\tau_{\min} = 0.01$  to prevent the chain from being trapped in regions with low acceptance. In the temperature annealing process, we begin with an initial temperature  $T_0 = 5$  and a cooling factor  $\zeta = 0.95$ , gradually reducing the temperature over time. The adaptation interval was set to  $N_{\text{adapt}} = 500$ , meaning the temperature was updated every 500 iterations according to  $T_n = \max(1, T_0 \zeta^{\lfloor n/N_{\text{adapt}} \rfloor})$ . The target acceptance rate was chosen as  $r_{\text{target}} = 0.40$ , and the step size  $\tau$  was adjusted adaptively to maintain this target rate. For burn-in,  $B = 7,000$  samples were discarded for the standard elliptic problem and  $B = 15,000$  for the fractional elliptic problem. The typical acceptance rate during the stable period ranges from 38% to 42%, ensuring effective exploration of the posterior distribution while maintaining computational efficiency.

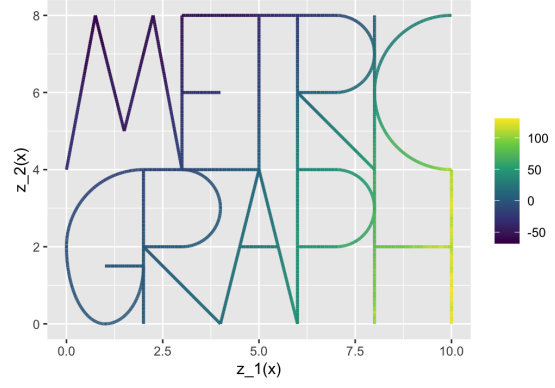
## 5.2 Elliptic Problem on a Letter-shaped Metric Graph

Here, we evaluate the performance of the MAP and posterior mean estimators of the ground-truth parameter  $u_0$ . We also evaluate the accuracy of the estimators of the ground-truth solution  $p_0$  obtained by applying the forward map to the MAP and posterior mean estimators of  $u_0$ . Figure 1 shows the posterior mean and MAP estimate alongside the ground-truth parameter  $u_0$ . Both estimators successfully recover the global structure of  $u_0$ , with only minor discrepancies at a few localized points. The corresponding PDE solutions also exhibit close agreement, except near the edges in which the ground-truth solution  $p_0$  attains large values. To assess uncertainty, Figure 2 displays the posterior marginal standard deviations. Regions with larger reconstruction errors coincide with elevated marginal standard deviations, confirming that the Bayesian approach correctly identifies areas of increased uncertainty.

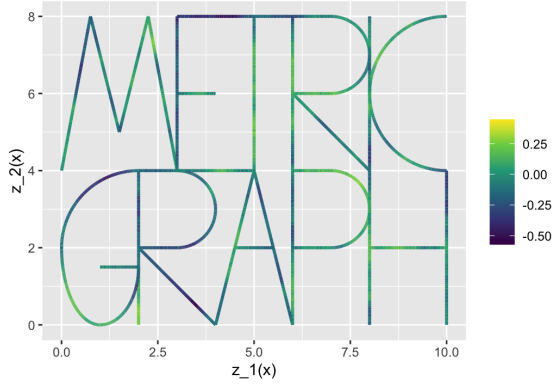
### Elliptic problem: estimates for parameter and PDE solution



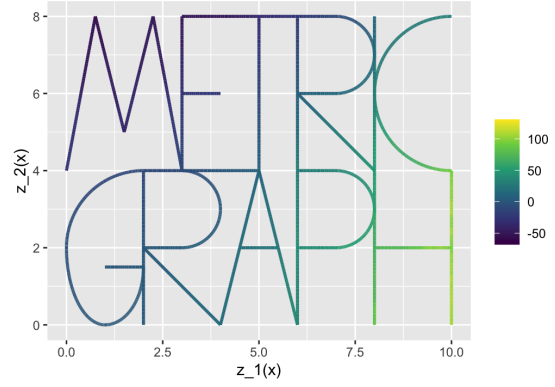
(a) Ground truth  $u_0$



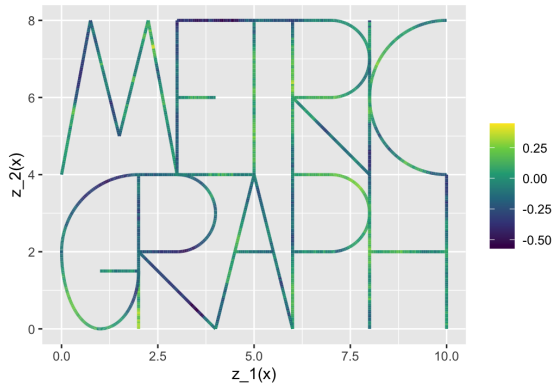
(b) True solution  $p_0$



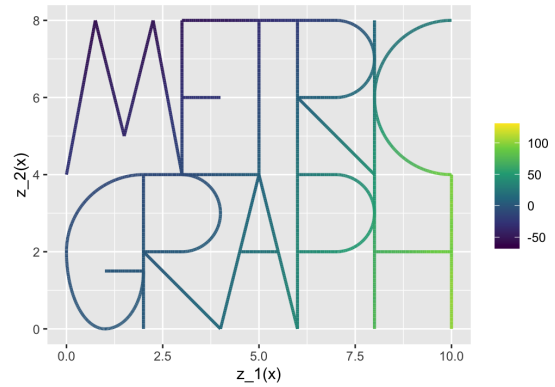
(c) Posterior mean estimate of  $u_0$



(d) Posterior estimate of  $p_0$



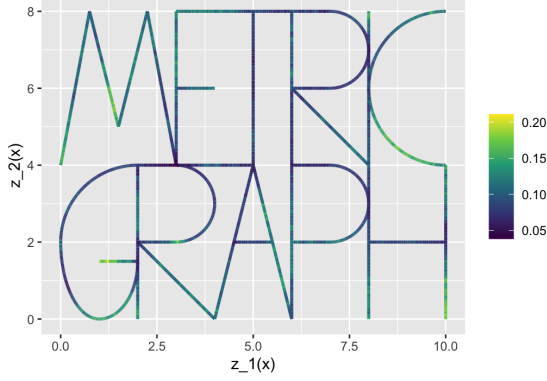
(e) MAP estimate of  $u_0$



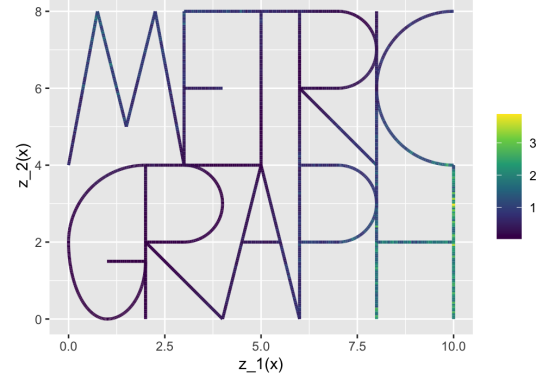
(f) MAP estimate of  $p_0$

Figure 1: Elliptic problem ( $\beta = 1$ ). Comparison of ground truth, posterior mean, and MAP estimate for the parameter (left column) and for the corresponding PDE solution (right column).

### Elliptic problem: posterior marginal standard deviation

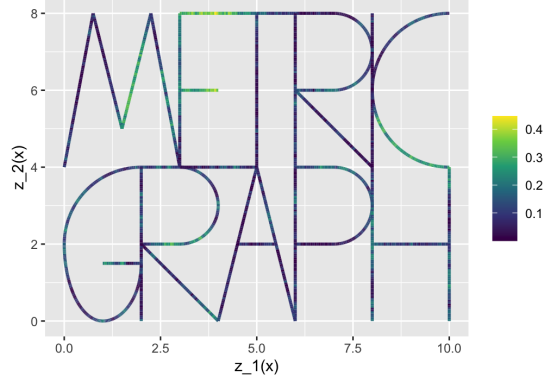


(a) Standard deviation for parameter

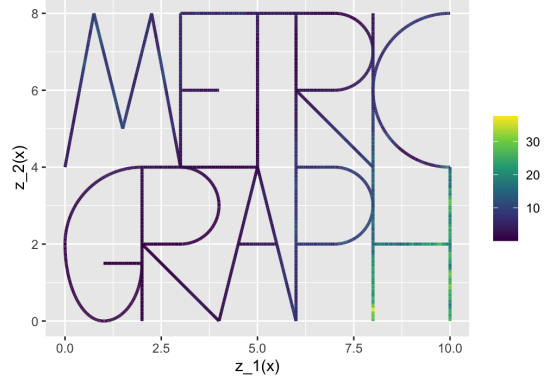


(b) Standard deviation for PDE solution

### Elliptic problem: absolute difference between truth and posterior mean



(c) Difference between truth  $u_0$  and posterior mean



(d) Difference between truth  $p_0$  and posterior mean

Figure 2: Elliptic case ( $\beta = 1$ ). Top row: posterior marginal standard deviation computed from MCMC samples for the parameter (left) and for the corresponding PDE solution (right). Bottom row: difference between the truth and the posterior mean for the parameter (left) and the PDE solution (right).



### 5.3 Fractional Elliptic Problem on a Letter-shaped Metric Graph

For the fractional elliptic case, we set the regularity parameter  $\beta = 3/2$  and follow the same workflow as in Subsection 5.2. Figure 3 shows strong agreement between the MAP and posterior mean estimators and the ground-truth parameter, with the RMSE falling below 0.08. Figure 4 displays the posterior marginal standard deviation computed from the MCMC samples; as in the elliptic case, regions of high marginal standard deviations match with regions of higher reconstruction errors.

## 6 Conclusions

This paper has studied the formulation, well-posedness, and numerical solution of Bayesian inverse problems on metric graphs, focusing on elliptic and fractional elliptic inverse problems. We have leveraged recent Gaussian process models on metric graphs to specify the prior, and we have built upon recent regularity theory for PDEs on metric graphs to establish the stability of the forward model. Numerical results demonstrate accurate reconstruction and effective uncertainty quantification.

Several research directions stem from this work, including: (1) Analyzing Bayesian inversion for other PDEs on metric graphs, which will likely require new regularity theory and stability estimates. (2) Developing prior models on metric graphs [5], including for instance level-set techniques for geometric inverse problems [23]. (3) Studying the effect of numerical discretization of the forward model and the prior in the posterior [33, 34]; doing so will motivate the design and analysis of new solvers for PDEs on metric graphs.

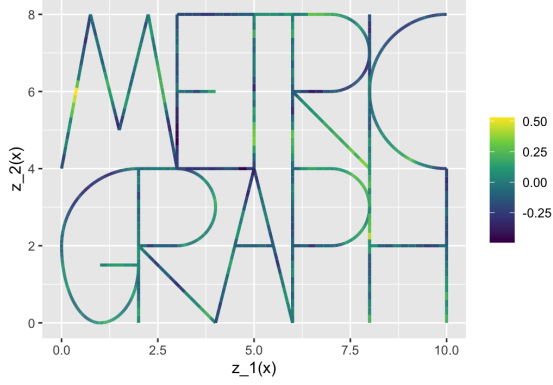
## Acknowledgments

DB was partially funded by King Abdullah University of Science and Technology (KAUST) under Award No. ORFS-CRG12-2024-6399. DSA was partly funded by NSF CAREER DMS-2237628.

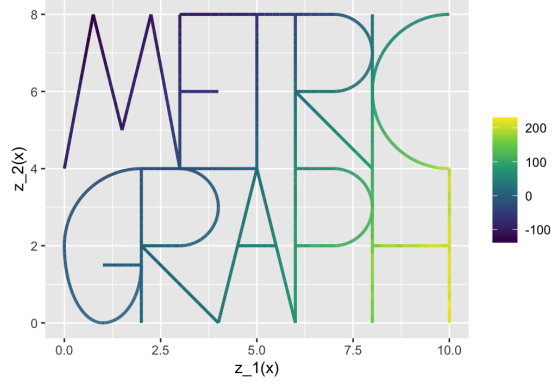
## References

- [1] G. BERKOLAIKO AND P. KUCHMENT, *Introduction to Quantum Graphs*, no. 186, American Mathematical Society, 2013.
- [2] D. BOLIN AND K. KIRCHNER, *The rational SPDE approach for Gaussian random fields with general smoothness*, Journal of Computational and Graphical Statistics, 29 (2020), pp. 274–285.
- [3] D. BOLIN, M. KOVÁCS, V. KUMAR, AND A. SIMAS, *Regularity and numerical approximation of fractional elliptic differential equations on compact metric graphs*, Mathematics of Computation, 93 (2024), pp. 2439–2472.
- [4] D. BOLIN, L. RIERA-SEGURA, AND A. B. SIMAS, *A new class of non-stationary Gaussian fields with general smoothness on metric graphs*, arXiv preprint arXiv:2501.11738, (2025).
- [5] D. BOLIN, D. SADUAKHAS, AND A. B. SIMAS, *Log-Gaussian Cox processes on general metric graphs*, arXiv preprint arXiv:2501.18558, (2025).
- [6] D. BOLIN, A. SIMAS, AND J. WALLIN, *Statistical inference for Gaussian Whittle-Matérn fields on metric graphs*, arXiv preprint arXiv:2304.10372, (2023).
- [7] D. BOLIN AND A. B. SIMAS, *rSPDE: Rational Approximations of Fractional Stochastic Partial Differential Equations*, 2025. R package version 2.5.1.
- [8] D. BOLIN, A. B. SIMAS, AND J. WALLIN, *MetricGraph: Random Fields on Metric Graphs*, 2023. R package version 1.4.1.

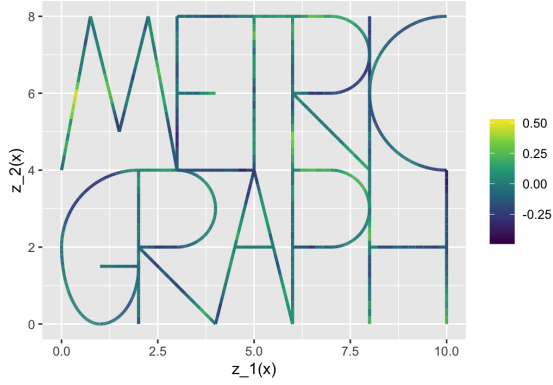
### Fractional elliptic problem: estimates for parameter and PDE solution



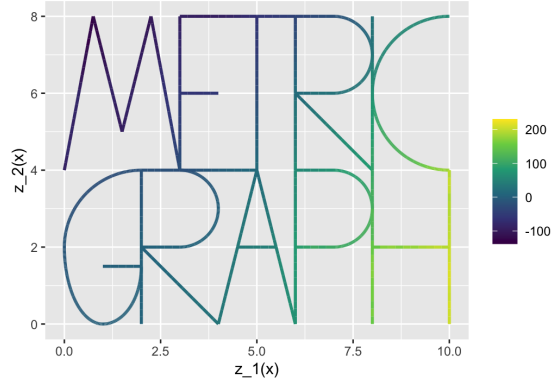
(a) True parameter  $u_0$



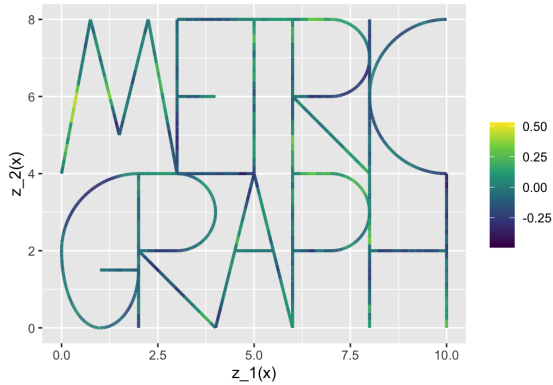
(b) True solution  $p_0$



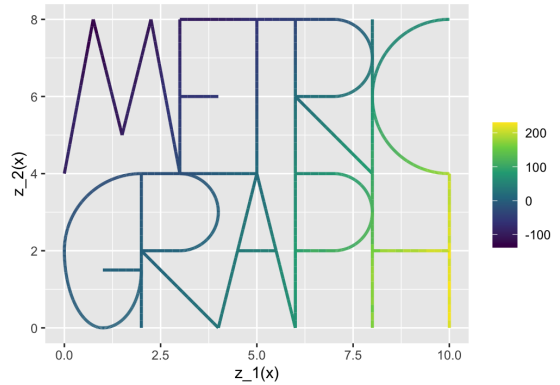
(c) Posterior mean estimate of  $u_0$



(d) Posterior mean estimate of  $p_0$



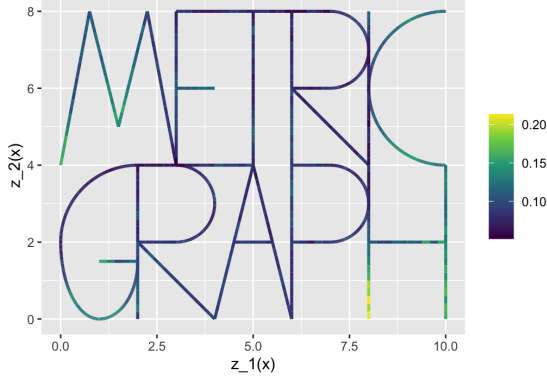
(e) MAP estimate of  $u_0$



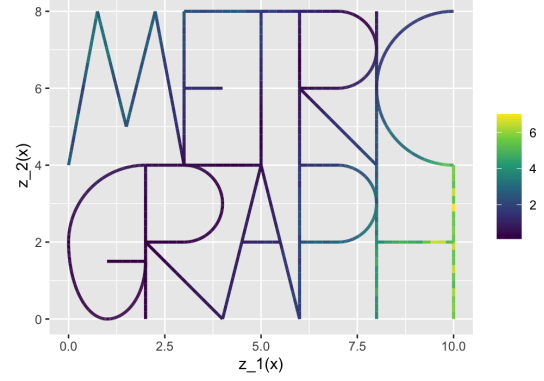
(f) MAP estimate of  $p_0$

Figure 3: Fractional elliptic problem ( $\beta = 3/2$ ). Comparison of ground truth, posterior mean, and MAP estimate for the parameter (left column) and for the corresponding PDE solution (right column).

### Fractional elliptic problem: posterior marginal standard deviation

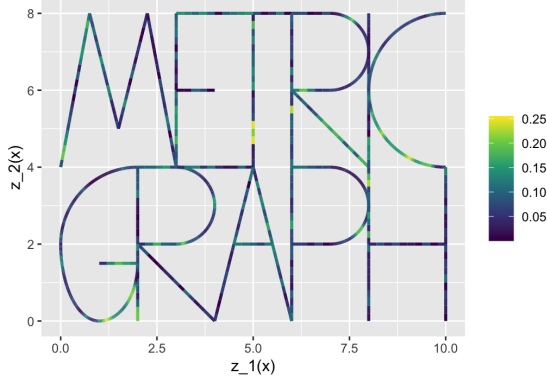


(a) Standard deviation for parameter

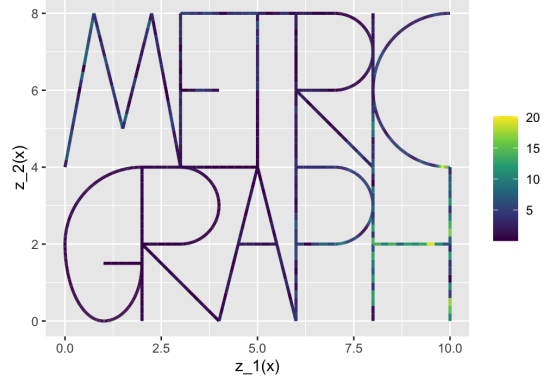


(b) Standard deviation for PDE solution

### Fractional elliptic problem: absolute difference between truth and posterior mean



(c) Difference between truth  $u_0$  and posterior mean



(d) Difference between truth  $p_0$  and posterior mean

Figure 4: Fractional elliptic problem ( $\beta = 3/2$ ). Top row: posterior marginal standard deviation computed from MCMC samples for the parameter  $u$  (left) and for the corresponding PDE solution  $p$  (right). Bottom row: difference between the truth and the posterior mean for the parameter (left) and the PDE solution (right).

- [9] D. BOLIN, A. B. SIMAS, AND J. WALLIN, *Gaussian Whittle–Matérn fields on metric graphs*, Bernoulli, 30 (2024), pp. 1611–1639.
- [10] D. CALVETTI AND E. SOMERSALO, *An Introduction to Bayesian Scientific Computing: Ten Lectures on Subjective Computing*, vol. 2, Springer, 2007.
- [11] S. L. COTTER, G. O. ROBERTS, A. M. STUART, AND D. WHITE, *MCMC methods for functions: Modifying old algorithms to make them faster*, Statistical Science, 28 (2013).
- [12] R. COURANT AND D. HILBERT, *Methods of Mathematical Physics. Volume I*, Wiley Classics Library, Interscience Publishers (John Wiley & Sons), New York, 2nd rev. English ed., 1953. Reprinted with corrections, 1989.
- [13] M. DASHTI AND A. M. STUART, *Uncertainty quantification and weak approximation of an elliptic inverse problem*, SIAM Journal on Numerical Analysis, 49 (2011), pp. 2524–2542.
- [14] ———, *Bayesian approach to inverse problems*, Handbook of Uncertainty Quantification, (2017), pp. 311–428.
- [15] E. B. DAVIES, *Spectral Theory and Differential Operators*, Cambridge Studies in Advanced Mathematics, Cambridge University Press, 1995.
- [16] N. GARCIA TRILLOS, Z. KAPLAN, T. SAMAKHOANA, AND D. SANZ-ALONSO, *On the consistency of graph-based Bayesian semi-supervised learning and the scalability of sampling algorithms*, Journal of Machine Learning Research, 21 (2020), pp. 1–47.
- [17] N. GARCIA TRILLOS AND D. SANZ-ALONSO, *The Bayesian formulation and well-posedness of fractional elliptic inverse problems*, Inverse Problems, 33 (2017), p. 065006.
- [18] ———, *Continuum limits of posteriors in graph Bayesian inverse problems*, SIAM Journal on Mathematical Analysis, 50 (2018), pp. 4020–4040.
- [19] N. GARCIA TRILLOS, D. SANZ-ALONSO, AND R. YANG, *Mathematical foundations of graph-based Bayesian semi-supervised learning*, Notices of the American Mathematical Society, 69 (2022).
- [20] M. HAIRER, A. STUART, AND S. VOLLMER, *Spectral gaps for a Metropolis–Hastings algorithm in infinite dimensions*, The Annals of Applied Probability, 24 (2014), pp. 2455–2490.
- [21] J. HARLIM, S. W. JIANG, H. KIM, AND D. SANZ-ALONSO, *Graph-based prior and forward models for inverse problems on manifolds with boundaries*, Inverse Problems, 38 (2022), p. 035006.
- [22] J. HARLIM, D. SANZ-ALONSO, AND R. YANG, *Kernel methods for Bayesian elliptic inverse problems on manifolds*, SIAM/ASA Journal on Uncertainty Quantification, 8 (2020), pp. 1414–1445.
- [23] M. A. IGLESIAS, Y. LU, AND A. M. STUART, *A Bayesian level set method for geometric inverse problems*, Interfaces and Free Boundaries, 18 (2016), pp. 181–217.
- [24] J. KAIPO AND E. SOMERSALO, *Statistical and Computational Inverse Problems*, Springer, 160 (2006).
- [25] H. KIM, D. SANZ-ALONSO, AND R. YANG, *Optimization on manifolds via graph Gaussian processes*, SIAM Journal on Mathematics of Data Science, 6 (2024), pp. 1–25.

- [26] P. KUCHMENT, *Graph models for waves in thin structures*, Waves in Random Media, 12 (2002), p. R1.
- [27] ———, *Quantum graphs: an introduction and a brief survey*, in Analysis on Graphs and Its Applications, vol. 77 of Proceedings of Symposia in Pure Mathematics, American Mathematical Society, Providence, RI, 2008, pp. 291–312.
- [28] J. LATZ, *On the well-posedness of Bayesian inverse problems*, SIAM/ASA Journal on Uncertainty Quantification, 8 (2020), pp. 451–482.
- [29] W. MCLEAN, *Strongly Elliptic Systems and Boundary Integral Equations*, Cambridge University Press, Cambridge, 2000.
- [30] A. ODŽAK AND L. ŠĆETA, *On the Weyl law for quantum graphs*, Bulletin of the Malaysian Mathematical Sciences Society, 42 (2019), pp. 119–131.
- [31] D. SANZ-ALONSO AND O. AL-GHATTAS, *A First Course in Monte Carlo Methods*, arXiv preprint arXiv:2405.16359, (2024).
- [32] D. SANZ-ALONSO, A. M. STUART, AND A. TAEB, *Inverse Problems and Data Assimilation*, vol. 107, Cambridge University Press, 2023.
- [33] D. SANZ-ALONSO AND N. WANIOREK, *Analysis of a computational framework for Bayesian inverse problems: Ensemble Kalman updates and MAP estimators under mesh refinement*, SIAM/ASA Journal on Uncertainty Quantification, 12 (2024), pp. 30–68.
- [34] D. SANZ-ALONSO AND R. YANG, *Finite element representations of Gaussian processes: Balancing numerical and statistical accuracy*, SIAM/ASA Journal on Uncertainty Quantification, 10 (2022), pp. 1323–1349.
- [35] ———, *The SPDE approach to Matérn fields: Graph representations*, Statistical Science, 37 (2022), pp. 519–540.
- [36] A. M. STUART, *Inverse problems: a Bayesian perspective*, Acta Numerica, 19 (2010), pp. 451–559.